1957

An investigation of a method of increasing the mach number range of a subsonic wind tunnel by means of an internal nozzle in the test section.

Roland, Harold E.

University of Minnesota, 1957.

http://hdl.handle.net/10945/24753

AN INVESTIGATION OF A METHOD OF INCREASING THE MACH NUMBER RANGE OF A SUBSONIC WIND TUNNEL BY MEANS OF AN INTERNAL NOZZLE IN THE TEST SECTION

A Thesis
Submitted to the Graduate Faculty
of the University of Minnesota

by

Harold E. Roland, Jr.
Major U.S. Marine Corps

In Partial Fulfillment of the Requirements
for the Degree of
Master of Science in Aeronautical Engineering
June 1957

ACKNOWLEDGMENTS

The author wishes to express his appreciation to Professor John D. Akerman for his interest and advice; to Mike Schonberg and Kjell Bengtsson for their invaluable suggestions and aid in skillful construction of the equipment; to the U. S. Naval Postgraduate School for sponsoring the attendance of the author at the University of Minnesota during this period of study; and to his wife for her understanding and encouragement throughout the entire period of the author's postgraduate study.

H. E. R.

TABLE OF CONTENTS

SYMBOLS

A_f	Area of the Foil Test Section	Ft^2
M_1	Mach number in the Foil Test Section	
p	Static Pressure	Lbs/Ft^2
p_o	Total Pressure	Lbs/Ft^2
q	Dynamic Pressure	Lbs/Ft^2
R	Gas Constant	$\frac{Ft\text{-}Lb}{Slug}{}^oR$
T	Static Temperature	^oR or ^oF
T_o	Total Temperature	^oR or ^oF
V_o	Velocity far Ahead of the Test Section	Ft/Sec
V_1	Velocity in the Foil Test Section	Ft/Sec
ρ	Density	$Slugs/Ft^3$
η	Efficiency of the Diffuser	
θ	Half Angle of Expansion of the Diffuser	Degrees

AN INVESTIGATION OF A METHOD OF INCREASING THE MACH NUMBER RANGE OF A SUBSONIC WIND TUNNEL BY MEANS OF AN INTERNAL NOZZLE IN THE TEST SECTION

SUMMARY

A method was sought to increase the Mach number range of a subsonic wind tunnel while utilizing the same maximum power, by the installation of a suitably shaped, removable nozzle in the test section.

Two foils were constructed and mounted vertically in the test section. These foils were shaped with their interior surfaces presenting to the flow a contraction, a short straight test section, and a pressure recovery diffuser. The exterior of the foils presented to the flow a gradual contraction to the trailing edges. Total and static pressures were measured around these foils through the complete range of the tunnel velocities. These foils were moved to four positions within the tunnel test section so that an indication would be given of the most favorable position for the Mach number increase. Complete contractions and diffusers were built around the four foil positions, and comparisons drawn between Mach number increases in these configurations and those achieved with the foils alone. Models of all configurations were also run in a two dimensional smoke tunnel

in an attempt to visualize the general character of the flow.

Mach number increases were achieved in excess of those computed by the incompressible form of the continuity equation, with the largest increase being indicated with a foil test section of a width of approximately 19 inches. These Mach numbers were greater than those which developed with complete contractions of the same test section width. The low Mach numbers with complete contraction and diffuser were due to the large losses in the diffuser. It did not appear practical to build efficient diffusers as the construction would be very extensive. The optimum position of the foils when the area of the test section was considered as an influencing factor, was at a position at or near the walls.

The maximum Mach number increase was from .245 to .309 or a 26.67 percent increase, with test section width decrease from 54 inches to 19 inches. This large increase was possible because of a boundary condition across the trailing edges of the foils which equalized the static pressure at the trailing edge. This forced a contraction of the flow ahead of the foils so that more mass flow passed between them and less outside, thus giving an increase in the velocity that was presented to the leading edge of the interior foil area.

It should be remembered that this was a problem to devise a method of Mach number increase that was removable from existing wind tunnel test sections, and not an investigation of a method to build new test sections with necessary modifications of contraction and diffuser.

RESULT SUMMARY

All Results with Same Maximum Available Power

All Velocities In Ft/Sec

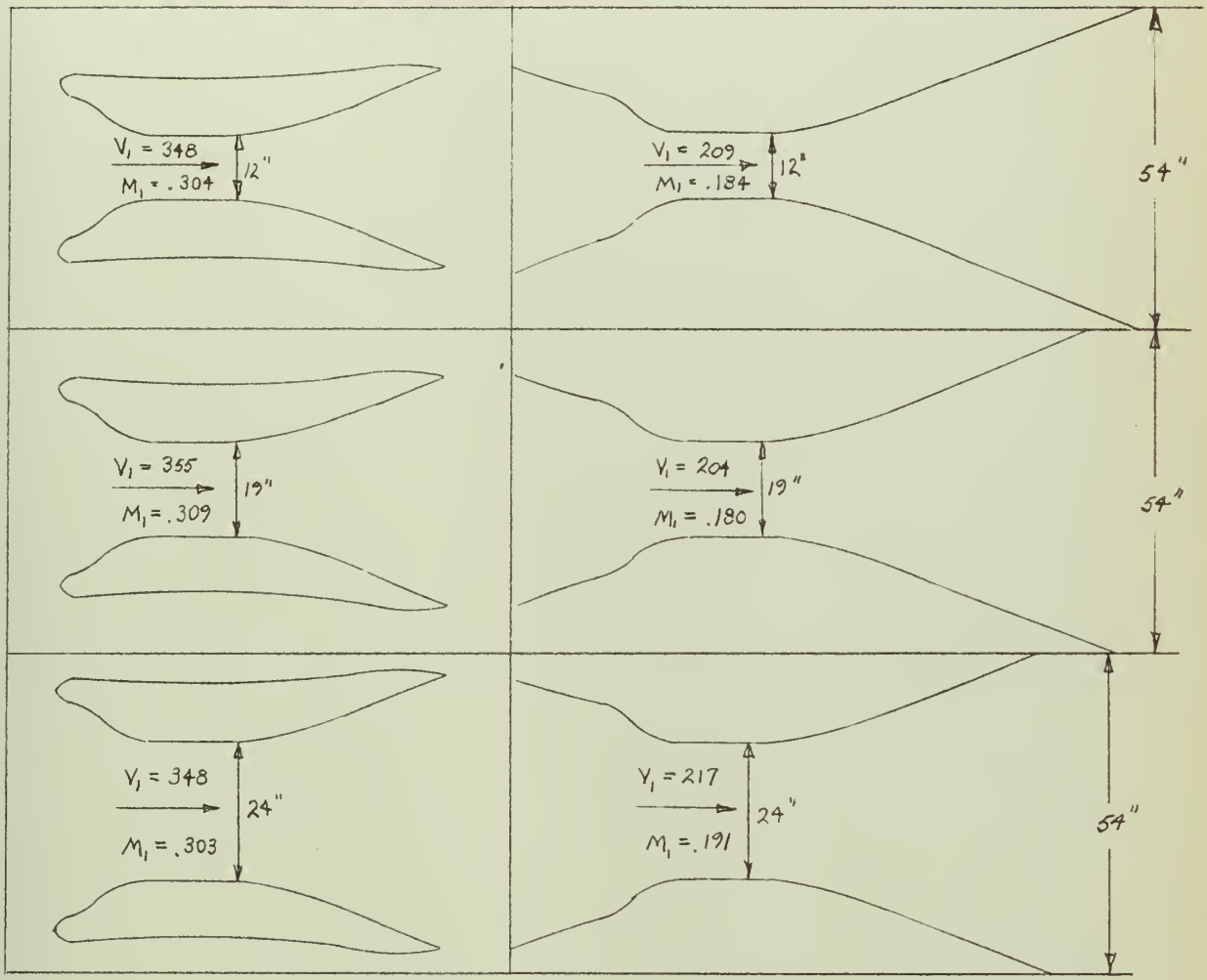

Normal Tunnel Test Section

Area of Normal Tunnel Test Section Reduced by the Projected Area of the Foils (Foils Mounted on the Walls)

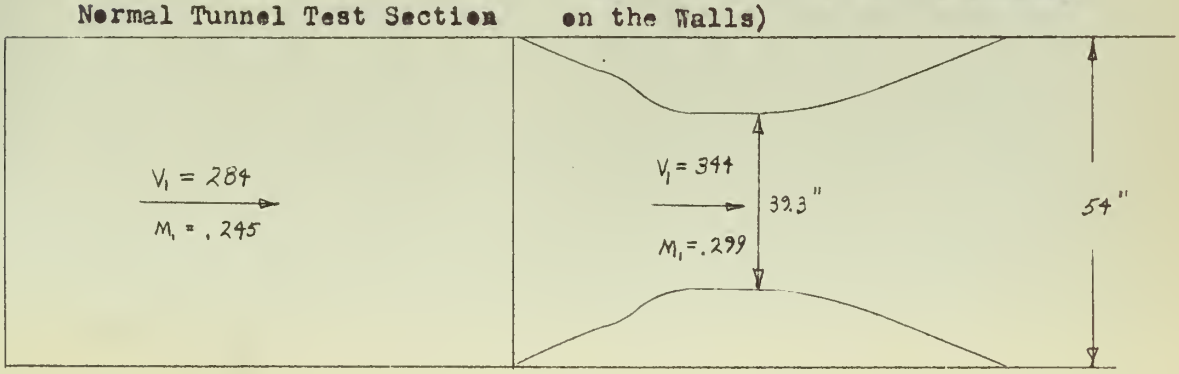

INTRODUCTION

In December of 1954, Dr. Rudolf Herman of the University of Minnesota completed a report on a supersonic wind tunnel called the "Ram Tunnel". This report was a research study for the Air Force and was written in response to papers by Dr. E. Steinhoff and Dr. G. Eber in which they discussed the possibility of extending the present potential of the supersonic sled. It was proposed that a ram-jet supersonic tunnel combination be mounted on a supersonic sled which would be driven by rockets. The Mach number of such a sled would be limited by a number of factors such as the length of the track and the braking efficiency. Dr. Herman showed that in the test section of the supersonic tunnel mounted on such a sled, a Mach number could be obtained which would be much higher than that of the sled. Specifically at a sled Mach number of 2.2 a Mach number within the test section of 4.0 could be expected. Such a "Ram tunnel" could also be mounted within the test section of a supersonic tunnel and if large enough, tests could be conducted in the greater Mach number range of the interior tunnel. Such a tunnel model was built for the purpose of testing the flow characteristics of the sled mounted "Ram Tunnel" and tested in a supersonic tunnel at the Rosemount Aeronautical Laboratories of the University of Minnesota.

Following this line of thought, it seems possible that the Mach number range of a subsonic tunnel could be extended by means of a suitable nozzle mounted within the test section. It is well known that the Mach number of a subsonic tunnel may be extended by means of an additional contraction built into the test section. However such contractions are usually quite restricted by the geometry of the tunnel. Because of the necessity for a smooth contraction of the flow ahead of the new test section, and for a diffuser with small angles of diffusion behind the new test section, the amount of contraction that can be built into the normal closed circuit tunnel is limited if losses are to be kept to a reasonable level. Furthermore such a contraction will cause additional drag in spite of the best design, and this drag will of course necessitate more power at the same V_o ahead of the test section. And since it is the extension of the maximum velocity of the tunnel that is of greatest interest, and since at that velocity the tunnel is already using the maximum power available, it is to be expected that a simple contraction would not be as advantageous as it would first seem to be.

In Ref. 2 reference is made to two dimensional jet inserts that have sometimes been inserted in the test sections of subsonic tunnels. These consist of

two vertically mounted plates between which may be suspended a two dimensional model. This insert has the advantages of reducing the turbulence of the flow and providing an easy method of mounting a two dimensional model.

Consideration was given whether or not to build a complete three dimensional test section within the original tunnel, or merely to build a two dimensional nozzle similar to the jet insert. It was decided that for an initial study such as this it would be advantageous to investigate the simplest form which might in the end turn out to be most useful.

Therefore combining the above ideas two foils were constructed and placed vertically in the test section of the Aero-Lab subsonic tunnel of the University of Minnesota. Their interior sides consisted of a contraction to a short straight area which could be considered the test section, and then expansion through a diffuser to the downstream end of the test section of the main tunnel. The exterior surfaces consisted of a slight contraction to the downstream end of the main tunnel test section. The foils were readily movable so that the area of the foil test section (A_f) could be varied.

Comparisons were made of the velocities and Mach numbers within this nozzle to those within the simple

contractions with test section areas comparable to those of the nozzle. These contractions were of necessity built around the foils. In addition, pressure measurements were made around the foils and an attempt was made to analyze the type of flow that occurred around them. The character of this flow was compared to that which was observed in a two dimensional smoke tunnel.

EQUIPMENT

Wind Tunnel

The basic piece of investigative equipment was the subsonic wind tunnel of the University of Minnesota. This was a closed circuit tunnel designed by the Aerolab Development Company and assembled at the University of Minnesota. Power for the tunnel was furnished by a 100 horsepower, 1200 RPM electric motor driving a variable pitch propeller. The airspeed in the tunnel is controlled by varying the pitch of the blades of the propeller. The test section of the tunnel is 38 inches high, 54 inches wide, and 58 inches in length. The two vertical sides of the test section are provided with glass doors for viewing the test in progress. These side panels are hinged to permit access to the test section. The tunnel airspeed is determined by two piezometer rings, each consisting of four orifices. One ring is located in the settling chamber and the other at the upstream end of the test section.

For the purposes of these tests, a fahrenheit thermometer was inserted in the settling chamber of the tunnel. This thermometer was assumed to read total temperature in the test section. This assumption would be true if the flow was adiabatic and the

thermometer read total temperature in the settling chamber. The mass flow rate through the tunnel is quite high in comparison to the amount of area through which heat may be transferred. In addition the temperature difference between the interior and exterior of the tunnel was not large. Therefore it can be assumed that relatively little heat was transferred from the flow, and the assumption of adiabatic flow appears to be valid. The thermometer was inserted approximately four inches into the flow of the settling chamber. As the flow in the settling chamber was only of the order of 40 feet per second at the maximum velocity of the tunnel, the thermometer could be considered as reading the total temperature of the flow in the settling chamber and thus in the test section.

Multiple Manometer

A multiple manometer was employed to measure pressures during the tests. This manometer was of the standard type with an adjustable reservoir supplying fluid to a series of tubes. Alcohol was the fluid used in this manometer, colored with flourescent type sea dye marker. This dye had the advantage of coloring the alcohol with the absolute minimum of added foreign matter and thus keeping the specific gravity of the alcohol unchanged. Also if any evaporization had taken place during the tests, the tiny percentage

of the dye would leave the specific gravity unchanged after the evaporization. To hold the evaporization to a minimum during the period of the tests, all of the manometer tubes not in use were capped. Those in use were capped between each test.

The manometer tubes were backed with graph paper with ten divisions to the half inch so that heights of columns could be read to the hundredths of an inch.

U-Tube Manometer

The airspeed of the tunnel was read on a U-tube manometer, the ends of which were connected to the two piezometer rings. This manometer was filled with a red oil base fluid which did not evaporate during the period of the test. This manometer was backed with graph paper with ten divisions to the half inch and the difference in fluid height could be quickly computed to the hundredths of an inch and converted to q in pounds per square foot.

Pitot Tubes

Three pitot static tubes were constructed as shown in Fig. 1 from specifications given in Ref. 3. These tubes were used throughout the experiment for measuring total and static pressures around the foils. The tubes could be screwed to the floor of the test section at any desired location. The horizontal center plane of the test section bisected the space between the total

and static tubes. Hoses led from connections at the base of the tubes along the floor of the test section to the tunnel vent at the rear of the test section and thence to the multiple manometer.

Foils

Two foils were constructed so that when mounted vertically in the test section of the tunnel they would present the following surfaces to the flow: on their interior surfaces a smooth contraction to a short straight section which could be considered a two-dimensional test section, and then expansion through what could be considered a pressure recovery diffuser. The exterior surfaces presented a continuous contraction to a point just ahead of the trailing edge and from there a slight expansion to the trailing edge. This is necessary if the flow is to be discharged over a knife edge in a direction parallel to the walls of the tunnel. The leading edge of the foils was rounded so that streamlines could strike it at any angle or any position and not flow around a sharp corner.

An inspection of Refs. 6, 7, 8, and 9 showed that all existing methods of contraction design are based on a given wall geometry or velocity distribution along this given geometry. As it was planned to vary the contraction ratio of the foils, it can be seen

that no analytic method of contraction design available in the literature would apply. However, velocity ratios of the foils mounted separately were expected to be of the order of two to one. And velocity ratios over this contraction, when the foils were mounted with full contraction installed to the tunnel walls, were expected to be much higher than two to one. Designing for the condition which it was hoped to maximize, a contraction with a velocity ratio of two to one was selected from Ref. 9. The coordinates of this contraction were taken from Ref. 9 and the x coordinates reduced by a factor of 1/5.2. This was necessary to keep the foil within the bounds of the test section of the main tunnel.

The straight portion of the foils was made long enough to at least approach a practical test section. Since the success or failure of this experiment was dependent to a large extent upon the geometrical restrictions of the situation, it was felt that it would be necessary to approach as near as possible a model that would have some real practical use.

The diffuser had an average half expansion angle of 16 degrees. This is much greater than that recommended in Ref. 4 which was 6.5 degrees for a diffuser consisting of two parallel walls and two diverging walls. However, to have an appreciable contraction

and still keep the foils within the length of the tunnel test section, it was necessary to have a diffuser angle this large.

Slots were cut through the foils at a point 4.75 inches from their trailing edge. The foils were solid at this position and the slots were cut through the solid wood the entire width of the foil except for the ribs as shown in Fig. 2. Holes were constructed diagonally through the foils from a point 14.2 inches from the trailing edge on the exterior surface to a point 15.4 inches from the trailing edge on the interior surface. These are also shown in Fig. 2. As the foils were hollow shells at this location, the holes were made by drilling diagonal holes through the surface of the foils and inserting brass tubes. These were later ground down to the surface of the foils and finished into the surface. There were six slots 1/4" x 4 7/8". There were 37 holes of 3/8 inch inside diameter. The purpose of the slots and holes was to bleed high pressure air from the diffuser to the low pressure of the exterior surface. This suction from the diffuser was to prevent separation within the diffuser. This will be discussed at some length in the discussion portion of this report.

The foils were a ribbed construction covered with 3/8 inch hard three-plywood. The ribs were braced with

lateral members. The leading edge was a solid member faired smoothly into the skin. The trailing edge was a solid piece over which the plywood was glued. The surface was sanded smooth, sprayed with two coats of varnish, rubbed down and waxed. Each foil was secured to the floor and ceiling of the tunnel by two brackets on each surface. (See Fig. 3) The complete installation of the foils with pitot static tube installed is shown in Fig. 6.

For this experiment the foils were moved to four different positions. This was done simply by removing the screws from the brackets and sliding the foil to the new positions. The four positions were with the foil test section 12 inches wide, 19 inches wide, 24 inches wide, and the foils against the wall of the tunnel test section. Diagrams of these four positions appear in Figs. 3, 4, 5, and 11.

For the latter stages of the experiment, it was necessary to fill the sections of the tunnel ahead and behind the foils to form a complete supplementary test section with test section area the same as that of the foil installation with which it was being compared. The diffuser to the rear of the foils was constructed of plywood sheets 75 inches long. These sheets were fitted to the rear of the foils and then ran downstream into the main tunnel diffuser as shown

in Fig. 7. This diffuser had a half angle of expansion greater than five degrees but again, because of the geometry of the situation, it was simply not practical to construct a diffuser of greater efficiency.

The contraction ahead of the foils was constructed of sheet metal, curved as shown in Fig. 7. This contraction was started as far ahead of the foils as was possible without causing extensive damage to the main tunnel contraction surface. As the foils were moved to each of their three new positions, the contraction and diffuser were modified slightly.

Fig. 10 shows the complete contraction built into the foils from the upstream and downstream end. Fig. 12 shows the foils mounted on the wall of the tunnel test section from the upstream and downstream end. Figs. 7, 8, and 9 are diagrams of the contraction installation for the three positions.

Smoke Tunnel

A schematic drawing of the small two dimensional smoke tunnel of the University of Minnesota is shown in Fig. 13. One blower provides draft for the fire if the smoke is being provided by fire, and forces the smoke to the entrance of the tunnel. Another blower sucks the smoke through the tunnel.

Smoke was made by burning heavy rags in the pipe type generator of the smoke tunnel. Various types of

smoke making methods were tried such as dry ice and hot water, titanium tetrachloride, a liquid that makes a very heavy smoke upon being exposed to air, burning rotted wood, and burning tobacco, but all things considered none were as satisfactory as the burning rags. Of the other methods that gave a satisfactory smoke, each coated the surfaces of the tunnel with deposit that impaired the operation of the tunnel and was difficult to clean off.

The models that were used in the tunnel were cut from 5/32 inch brass sheet. They were cut to a scale that was closest to making the height of the smoke tunnel correspond to the width of the main tunnel test section. (5:1) To make the scale exact, it was necessary to insert small strips of metal along the edges of the smoke tunnel. These are visible in the pictures of the various smoke tunnel runs.

Fig. 14 is a picture of the smoke tunnel.

PROCEDURE

The experimental procedure furnished data for a comparison of the velocities within the foil test section to those within a contraction of the same area, and to those within a contraction that would be formed by the projected areas of the foils, over the entire velocity range of the tunnel. In addition, the flow over the foils (A_f = 12 inches) was analyzed in some detail and enough data taken from the other two positions of the foils to determine that the character of the flow in those positions was essentially the same as that in the position of the smallest foil test section. An attempt was also made to confirm the character of flow with a smoke tunnel.

The three foil test section widths selected were 12 inches, 19 inches, and 24 inches. These three widths were selected so that the smallest was a minimum for a two dimensional model and the largest did not place the exterior surfaces of the foils so close to the test section walls that the character of the flow would be changed.

Before tests were run, it was thought desirable to get some idea of the quality of the separation that was going to occur in the foil diffuser and the effect that the holes and slots were going to have on this separation. A single foil was placed in the position

shown in Fig. 15 and tuft photographs taken of the diffuser at an intermediate tunnel speed with the holes and slots open and the holes and slots closed. This foil was positioned as far from the wall of the test section as it would be from the center line of the test section when in its normal operating position. (A_f = 12 inches) One-half inch was added to this distance for boundary layer. The foil was then moved to its normal operating position and tuft photographs taken of the diffuser with the holes and slots open and the holes and slots closed. A diagram of this position is shown in Fig. 16.

Placing the foils in position with A_f being 12 inches, a pilot run was made to standardize settling chamber total temperatures at each V_o of the tunnel that would be used on all succeeding runs. These temperatures were selected in conjunction with certain pressure differences as read on the U-tube manometer connected to the piezometer rings. As the piezometer ring located in the test section was upstream of the leading edge of the foils, this pressure difference was the q of the test section and from it V_o of the foils could be calculated. An attempt was made to select temperatures that would occur naturally during the course of the readings, realizing that for the 12 inch A_f the heating would be most rapid due to the

greatest contraction ratio and that these temperatures could be met during the other runs by waiting longer periods of time between readings. The below schedule of the pressures in pounds per square feet and total temperatures in degrees fahrenheit, was followed in the recording of data wherever possible. This in effect fixed a set of V_os for which pressures could be recorded.

Total Temperature Degrees Fahrenheit	74	76	80	84	86	90	95
Pressure Difference U-Tube Manometer Lbs/Ft^2	12.50	20.90	25.38	29.60	33.90	38.10	42.30

During runs with A_f 19 and 24 inches, it was possible to achieve more than 42 pounds pressure difference between the settling chamber and the test section. Appropriate temperatures were selected for these higher readings.

It was noted that in previous experiments with this particular tunnel the velocity in the settling chamber had been assumed to be zero for the purposes of computing the velocity of the test section. It was necessary to know if this assumption was true. Removing the foils from the tunnel and placing a pitot static tube centered in the test section, the tunnel was run through its

entire range of velocities and the data plotted in Fig. 19. It can be seen that the assumption that the total pressure in the tunnel is equal to the static pressure in the settling chamber is quite valid until the higher tunnel velocities are approached, and that even at these higher velocities the assumption is within good experimental tolerances.

Placing the foils back in the tunnel with A_f equal to 12 inches, total and static pressures were recorded at the positions shown in Fig. 3 over the range of tunnel velocities. For the purposes of the detailed analysis of the flow, only three values of V_o were used, a low value, a maximum value, and an intermediate value.

Total Temperature Degrees Fahrenheit	76	86	95
Pressure Difference U-Tube Manometer Lbs/Ft^2	20.90	33.90	42.30

Three pitot static tubes were utilized in the recording of this data. All three were used during each run whenever it was possible to position them so that they would not influence the pressures being recorded on the other two.

At the beginning of each run the barometric pressure and temperature were recorded. This was done at

the beginning of each run as the tunnel heated the air in the vicinity of the barometer by as much as five degrees and this increase would not have been fully registered in the metal parts of the barometer by the end of the run, thus giving incorrect temperature correction factors as taken from the tables of Ref. 10. Pressures were read for each standard V_o when the corresponding standard temperature, less one to two degrees, was reached in the settling chamber. It was found that during the period of time that the data was being recorded the tunnel heated two degrees at the lower velocities and four degrees at the higher velocities. Following each run, it was necessary to allow the tunnel to cool for a minimum of one hour, the total time depending upon the temperature to which the room could be cooled. This was necessary to bring the tunnel settling chamber temperature down to 74 degrees fahrenheit.

When all data had been taken at A_f of 12 inches the foils were moved to an A_f of 19 inches and total and static pressures recorded at the positions indicated in Fig. 4. The foils were then moved to an A_f of 24 inches and pressures recorded as shown in Fig. 5. At each of these positions, the pressures were recorded over the entire range of the tunnel velocities. As the A_f became larger, it was possible to reach higher values of V_o due to the decreasing contraction ratio and losses.

The foils were then returned to the 12 inch A_f position and a contraction constructed to the leading edge of the foils as shown in Fig. 7. A single run was made without the diffuser for determination of the amount of loss that would be eliminated with the diffuser installed. The diffuser was then installed and the total and static pressures were recorded in each case as shown in Fig. 7. It was hoped that pressures could be recorded at the same three values of V_o that were used for the detailed analysis of the 12 inch foil separation. However, the lowest value of V_o used previously could not be reached with or without the diffuser installed. Therefore only one V_o was used, the maximum obtainable.

As the contraction covered the two wall static pressure orifices of the piezometer ring at the upstream end of the test section and thus modified the velocity that occurred at the floor and ceiling orifices, it was necessary to recompute the pressure differences that would occur between the settling chamber and test section so that equivalent V_os would be imposed upon the contraction. An example of these computations is made in the Appendix C for each of the four foil positions which had contractions which covered the piezometer openings.

When the data was complete for the 12 inch A_f, the contraction was dismantled, the diffuser removed and the foils moved to the 19 inch foil test section. A new contraction was constructed and the diffuser reattached. Total and static pressures were recorded at the points shown in Fig. 8 for a single value of V_o. A similar operation was carried out for the 24 inch A_f with data recorded at positions shown in Fig. 9. Upon completion of this last run, another tunnel calibration run was made. The floor and ceiling of the test section had been roughened by a large number of screw holes during the course of the tests. Although these had been covered with cellophane tape as they occurred, it was felt that perhaps some additional losses had been added to the tunnel during the course of the tests. The final calibration was identical to the first.

Following is a summary of the various foil arrangements that were used with number that may be used hereinafter in referring to them.

Tunnel Arrangement Number	
1	Foils mounted 12 inches apart ($A_f = 12$)
2	Foils mounted 19 inches apart ($A_f = 19$)
3	Foils mounted 24 inches apart ($A_f = 24$)
4	Foils mounted 12 inches apart with contraction

Tunnel Arrangement Number	
5	Foils mounted 12 inches apart with contraction and diffuser
6	Foils mounted 19 inches apart with contraction and diffuser
7	Foils mounted 24 inches apart with contraction and diffuser
8	Foils mounted on the walls with contraction

The Smoke Tunnel

In an attempt to lend support to the general character of flow that was theorized to have occurred in the main tunnel, a smoke tunnel was used.

The generation of the smoke proved to be a knotty problem. Several methods of smoke generation were tried without satisfactory results. Dry ice and hot water provided smoke that was too heavy and such a generator operated for only 40 seconds at which time the dry ice became coated with a layer of frozen water. Titanium tetrachloride was tried without success. The smoke generated coated the glass of the tunnel, the model, and the smoke holes with a white deposit which was difficult to remove. In addition, it was necessary to exhaust this smoke from the room in which the tunnel was running. This proved a difficult problem. Burning materials were tried with some success, burning rags proving to be the most satisfactory. Controlling the

amount of air that was used as draft for the generator, by either turning the draft motor on and off or by a valve in the air intake to the draft motor, the amount of smoke that was presented to the entrance of the tunnel could be well controlled. It was therefore possible to take pictures with the streamlines well defined as fine lines of smoke or broad bands.

The pictures were taken with a polaroid land camera with an f 4:5 lens, and flash. The black background of the tunnel absorbed most of the light of the flash. Therefore, although the smoke was dimly visible to the naked eye, the great overexposure that was necessary because of the dark background, caused the smoke to stand out sharply in the pictures.

Reflection from the glass surface of the tunnel was eliminated by attaching an extension cord to the flash attachment and positioning it so that the flash would not be reflected in the lens. Several positions of the flash were tried, to the side and below. A satisfactory location was found shining onto the models at a 30 degree angle from below. This low position kept the light from reflecting into the lens of the camera and provided satisfactory illumination of the model and smoke.

Models were run in the tunnel arrangement numbers one through eight.

RESULTS AND DISCUSSION

The results of this study are found in Tables I through VII and Figs. 17 through 39.

Analysis of the Holes and Slots

The holes and slots were installed in the foils to prevent separation in the diffuser by suction. These holes and slots were so installed that they ran from regions of high pressure in the diffuser to regions of lower pressure on the exterior of the foils. Calculations of these positions by incompressible theory appear in Appendix A.

One of the objects of this investigation was to achieve a Mach number in the test section of the foils that was in excess of that which could be achieved by the contraction ratio of the foils. If the holes and slots operated as they were designed to function, this Mach number increase would be achieved by the ejection of the high velocity air around a central wedge of slower air exiting from the foil diffuser, and by a lowering of the pressure in the foil diffuser over that which could be expected from the expansion ratio of the diffuser. One condition that could cause the holes and slots to operate incorrectly was a zero pressure differential across them, or a pressure differential directing the flow to the interior of the foils.

This latter condition is the one that occurred, as can be seen by examining Table I.

Table I shows the total and static pressures taken at points just opposite the entrances to the holes and slots as shown in Fig. 3. Total pressures are shown for the purpose of indicating where losses occurred. It can be seen that no losses occurred on the exterior of the foils or the interior of the right foil. It appears that the flow has separated entirely from the left foil but is clinging to the right foil. This will be discussed in detail later. The static pressure in all cases is less in the interior of the foils than the exterior. The cause of this undesirable pressure gradient is the boundary condition of equal static pressure immediately across the rear of the foils. In order to meet this boundary condition, the flow adjusts itself ahead of the foils by contracting the streamlines so that more mass flow goes between the foils than outside of them. Thus, although the holes and slots are not operating as designed, the very boundary condition that causes them to be useless creates a condition that gives the desired Mach number increase in another way. This will be discussed in detail in later paragraphs.

If in designing the foils it could have been assumed that the static pressure would equalize immediately across the rear of the foils, in addition to

making the usual assumption of no losses, then from Bernoulli's equation:

$$P_o = p + \frac{\rho}{2} V^2$$

The velocities would be equal across the rear of the foils. This of course would make any ejection action impossible. And since the static pressure will tend to propagate upstream, it will make it extremely unlikely that appreciable pressure differences will exist across the slots if not the holes. This condition of equal velocities occurs across the rear of the right foil because there is no loss in the interior of the right foil. This can be seen in Table II, a listing of the total and static pressures and the velocities and Mach numbers across the trailing edge of the right foil. The data was taken at the points near the trailing edge of the right foil shown in Fig. 3.

Table III is a listing of velocities and Mach numbers in the foil test section with various combinations of holes and slots open in the 12, 19, and 24 inch test sections. This table, together with Figs. 28, 29, and 30, which are plots of this table, show the effect of the holes and slots on the velocities and Mach numbers in the foil test sections. It can be seen that opening or closing the holes and slots has very little effect upon the flow in the test section of the foils.

An inspection of Figs. 17 and 18 offers further evidence of the ineffectiveness of the holes and slots. Fig. 17 was taken (as shown in Fig. 15) with the foil mounted near the window. The foil was mounted as far from the window as it would be from the center line of the flow in its normal position, with a half inch allowance for boundary layer. Flow in the pictures is from left to right. A close inspection shows that separation is starting with the first row of tufts as the shadows show that they are not lying on the surface of the foil. Further inspection shows that the turbulence is slightly higher in the case of holes and slots open. This would be expected with the flow from the openings toward the camera.

An inspection of Fig. 18 shows much less separation and turbulence with the foil in its normal position. No shadows are visible under the first two rows of tufts. This emphasizes a fact which was brought to light several times in this study and which is mentioned in the literature but not emphasized: namely, that the separation in a diffuser is a function not only of the angle of the diffuser but the expansion ratio.

Again in Fig. 18, the picture with the holes and slots closed, exhibits slightly less turbulence than the one in which they are open.

In view of the foregoing evidence, it was decided to complete the investigation with the holes and slots sealed with cellophane tape. For the remainder of the discussion the foils will be considered only with holes and slots closed.

Analysis of Mach Number Increase

One of the objects of this investigation was to achieve a velocity increase in excess of that which would be expected from the incompressible form of the continuity equation.

$$A_1V_1 = A_2V_2$$

$$V_2 = \frac{A_1V_1}{A_2}$$

where A_1/A_2 = contraction ratio

Figs. 31, 32, and 33 show that this increase was actually achieved. These figures show the velocity and Mach number plotted versus V_o compared to the velocity and Mach number versus V_o that could be expected from the incompressible form of the continuity equation with no losses. It can be seen that there is some variation in the increase as the foil test section width is varied. Fig. 34 is a plot of the maximum velocity and Mach number versus the test section width. Three points are insufficient to give a good curve but this figure shows that there is a definite tendency for the Mach numbers and velocities

to peak at certain foil test section widths and then fall off.

A quick look at Figs. 31, 32, and 33 shows that the percentage increase varies with the test section width and from low velocities to high velocities. Table IV shows the maximum, minimum, and mean percentage increase in velocity for each foil test section width. The maximum always occurs at the highest V_o and the minimum at the lowest V_o. Fig. 35 is a plot of the data in Table IV. It shows that the percentage increase goes up rapidly as the foil test section width is increased, then levels off and would of necessity fall to zero as the foils approach the wall where the entire mass flow must pass between them and there will be no boundary effects causing the increases. These boundary effects are discussed in following paragraphs.

From the foregoing information it is not apparent just where the most advantageous position would be for these foils in this wind tunnel. A percentage increase is not in itself any advantage and the maximum curves are not very conclusive. The two measures of the value of a wind tunnel which are considered here are Mach number and test section area. It might be arbitrarily stated that the Mach number is two, three, or four times as valuable a characteristic of the wind tunnel as the test section area. Then seeking a means of

evaluating wind tunnels in terms of Mach number and test section area, it could be said that the sum of twice the Mach number and another nondimensional number formed by dividing the reduced test section area by the full test section area, would be an indication of the relative worth of the five test sections considered in this investigation. These five sections are the three foil sections, the section formed by mounting the foils on the walls, which is merely reducing the tunnel test section by the projected area of the foils, and the full tunnel test section. Assuming that the Mach number of a wind tunnel might be worth two, four, six, ten, 15, and 20 times the tunnel area, the relative worth of the five test sections might be compared for each of these conditions. Test section numbers were formed for each of these conditions and plotted versus test section width in Fig. 36. It is evident from this method of comparison that reducing the tunnel by the projected area of the foils gives a more valuable test section. It would seem, therefore, that if a test section combining the best features of high Mach number and wide test section area is desired, it would be best to design a complete contraction that would decrease the original test section area by a modest amount.

As a means of comparing the velocity and Mach number increases achieved with the foils to that which

might be achieved if complete contractions of the same width as the foil test sections were built within the test section of the main tunnel, contractions were built ahead of the foils and diffusers behind for each test section width. It was originally intended that the tests would be run at each of the three standard V_os used previously and V_o maximum. It immediately became apparent that because of the extreme losses in the diffusers, the maximum V_o that could be reached would not be as high as the lowest of the three standard values. Therefore each run was made only at V_o maximum. Data was taken at the points as shown in Figs. 7, 8, 9, and 11. Only enough data was taken to give the velocity and Mach number in the test section and the general nature of the flow. Table V compares the velocities and Mach numbers in the test sections of the three contractions. It can be seen that there is little change in the velocity for the three different sections. It is interesting to note that when the 12 inch A_f was run without the diffuser the same velocity and Mach number were achieved as when the diffuser was added. This might have been anticipated if the nature of the flow had been considered. Heavy separation begins to occur in the foil diffuser before the trailing edge. This separated turbulent region continues on downstream into

the main tunnel diffuser. The placing of diffuser vanes along the walls of the tunnel at angles greater than the expansion ratio of the smooth flow will not appreciably decrease the losses in the flow. To make this diffuser effective, it would have been necessary to run the diffuser vanes not from the trailing edge of the foils, but from the straight test section area of the foils. The vanes would then have had to run downstream at angles of 6.5 degrees or less. This would necessitate building a supplementary diffuser almost the entire length of the main tunnel diffuser. Such extensive construction simply is not practical for the purpose of a small Mach number increase.

It is noted that as the test section area is varied, the Mach number remains constant. This conclusion can be reached from reasoning with an energy concept. The hundred horsepower can impart only a certain amount of energy to the flow. Then as the losses are decreased by increasing the test section area, this additional energy is available to be converted to Mach number. That increasing the test section does decrease the losses can be seen by the limiting case of the foils mounted on the wall. As shown in Table V, V_o is much higher, V_1 is higher, and the total pressure is higher with very little loss occurring near the trailing edge of the foils

near the interior surface. Therefore it would seem that increasing the test section width does decrease the losses. This decrease must be caused to a great extent by the previously mentioned theory that separation in a diffuser depends somewhat upon the expansion ratio. The diffuser in this case maintains the same angle but decreases the expansion ratio.

In conclusion, it might be stated that the building of new test sections with large contraction ratios within the main test section of a wind tunnel is not practical due to the extreme losses that will occur without extensive construction.

Analysis of the Flow (A_f = 12 inches)

As stated before, only in the case of the 12 inch foil test section was a detailed analysis and calculation of the flow attempted. It is believed that the general character of the flow was the same in the cases of the 19 and 24 inch foil test sections. Table III shows that the holes and slots effected little change in the velocity and Mach number of the flow in the cases of the 19 and 24 inch test sections, just as in the 12 inch test section. This would indicate that the static pressure is equalizing at the trailing edge of the foils in all three cases. Table VI is a summary of data taken ahead of the foils as shown in the table and in Figs. 4 and 5. Table VI shows that a contraction

is occurring ahead of the foils just as it will be shown that one is occurring in the case of the 12 inch test section. This contraction is indicated by the increase of velocity from a position 11.2 inches ahead of the foils to a position at the leading edge of the foils. Smoke tunnel pictures which will be considered in later paragraphs will show that separation is occurring in the diffuser of the 19 and 24 inch test sections just as in the 12 inch test section width.

In considering the flow in and around the foils, it seemed wise to start at the trailing edge because that is where the cause of the flow phenomenon lies. As was stated in the section on holes and slots, the flow in the interior of the foils seems to have separated from the left wall with large losses and was clinging to the right wall with relatively little loss. This fact is confirmed by a pressure survey taken at seven points across the diffuser of the foils at a point even with the trailing edge. The location of these data points is shown in Fig. 3. Fig. 37 is a plot of the velocities at this survey station. The three V_os are the standard ones used throughout this report. This figure confirms the fact that there is heavy separation occurring along the left foil, with reverse flow extending out to five inches from the foil surface. This separation from one wall is not

necessarily due to misalignment of the foils. Fig. 9 of Ref. 4 shows a picture of separation of this type when the diffuser has curved walls and the angle of the wall is over that specified for good efficiency.

The areas under the curves of Fig. 37 were integrated by Simpson's rule to give an integrated velocity which could be used in the continuity equation.

Fig. 38 is a plot of the static gage pressures across the trailing edge of the foil diffuser. This again bears out the extreme separation that occurs near the left foil. Integrating the areas under these curves will give integrated static gage pressures for each V_o.

A consideration of the diffuser efficiency will show how far the limits of good diffuser design were exceeded because of the geometric restrictions of the main tunnel test section. From Ref. 3, p. 52, the formula for the efficiency of a diffuser of an incompressible fluid is taken.

$$\eta = \frac{p_2 - p_1}{\frac{1}{2}V_1^2\left[1 - (A_1/A_2)^2\right]} \qquad p_2 = p_2 \text{ integrated}$$

The actual computation of the efficiencies is shown in appendix E. The efficiencies for the three standard V_os are, 53.1%, 51.2%, and 52.8%. Ref. 4, Fig. 4 shows an efficiency of 50 percent for a rectangular two dimensional diffuser with A_2/A_1 of four and

the angle of expansion at 30 degrees. A_2/A_1 in the case of the foils is about 4.5 with the angle of expansion about 32 degrees. Thus the efficiency of the foil diffuser is about what would be expected from previous work on diffusers. However, the experimental results cited in Ref. 4 are for straight walled diffusers and the foil walls are curved. Ref. 4 states that curved walls would tend to increase slightly the efficiency of a diffuser. In addition, the foil diffuser is not a simple diffuser but has flow around it. The flow on the exterior of the foils has a higher static pressure than that within the diffuser. As the static pressure attempts to equalize across the trailing edge of the foils, the higher exterior pressure would tend to increase the adverse pressure gradient in the diffuser, thus increasing the separation and lowering the efficiency of the diffuser. These two effects evidently cancel each other.

In summary, it can be said that the efficiency of the foil diffuser is about 50 percent and previous experimental results confirm that this is an approximately correct result for diffusers of this configuration. Highly efficient diffusers can be expected to have an efficiency of 80 percent.

From the low value of the diffuser efficiency, it would be expected that any velocity increase in the

foil test section would be extremely difficult to achieve and would certainly not be as great as the incompressible form of the continuity equation would indicate. However, Figs. 31, 32, 33, and 35 show that the velocities that would be expected from the continuity equation have been exceeded. The reasons for this can be found in the geometry of the foils and the boundary conditions that exist across the trailing edges. Incompressible theory will show that there should be a pressure difference across the trailing edge of the foils of 15.33 pounds per square foot, at a V_o of 195 feet per second. However, since an infinitesimal distance downstream of the foils' trailing edge the pressures attempt to equalize, the character of the flow ahead of the foils must change to meet this boundary condition. To decrease the pressure within the foils and increase it outside, it is necessary for more of the mass of the flow to go inside the foils. Considering the flow incompressible, this will increase the velocity throughout the interior of the foils and decrease the static pressure. And conversely, with less mass flowing outside the foils the velocity will be decreased and the pressure increased. This was accomplished by a contraction of the streamlines ahead of the foils so that the V_o that was presented to the leading edge of the foils was much greater than that which was measured by the piezometer holes. That this contraction actually occurred can be

seen in Table VI. This data was taken at the positions indicated in the table and Fig. 3. This type of a contraction is of course the most efficient for increasing the velocity of the flow because the streamlines form the perfect walls, causing no losses due to friction or separation.

With the above basic facts concerning the flow, an attempt was made to calculate the velocities of the flow at key locations around the foils as indicated in Table VII. The details of the calculations are shown in Appendix D. The calculations were started at the trailing edges of the foils and projected forward. The integrated velocity at the trailing edge of the foils was used and the assumption was made that the static pressures equalized across the trailing edges of the foils a short distance downstream. The velocities were projected from one area to another with the incompressible form of the continuity equation. Table VII shows the calculated velocities, the experimental velocities, and percentage error. Calculations were made separately along the left and right foils. It can be seen in Table VII that the agreement is good over the right foil. This is the foil along which there was no separation. This unsymmetrical condition at the rear of the foils distorted the contraction ahead of the foils so that although the velocity gradients were not large across the right half of the

entrance to the interior of the foils, large velocity gradients existed across the left half of the entrance and the contraction was not well defined ahead of the left foil. These large velocity gradients across the left half of the foil entrance account for the larger percentage errors in the velocity calculations for the left foil.

Smoke Tunnel Analysis

Figs. 20 through 27 are pictures of runs made in the smoke tunnel previously described. Pictures are included for each of the configurations tested in the wind tunnel. Two pictures of each configuration are shown, each with a slightly different degree of smoke for better analysis of the flow. Unfortunately the character of the flow in the smoke tunnel was not the same as it was in the wind tunnel. As can be seen in Fig. 13, the thickness of the test section is only 5/32 of an inch. This means that most of the flow is boundary layer.

However, certain things of interest can be seen. Looking first at the pictures of the foils alone, Figs. 20, 21, and 22, the separation in the diffuser is clearly evident. The decrease in the amount of separation can be seen as the foil test section is changed from 12 to 24 inches. In Figs. 21 and 22 smoke streams are so positioned that it is shown that the streamlines do

follow the contraction. Due to lack of smoke, it is not possible to say definitely in the 12 inch case, but it appears that the streamlines do not follow the contraction as closely as in the other two cases. The contraction of the streamlines ahead of the foils and the separation of the flow from one foil only, does not appear in these pictures.

Comparing the foils mounted with the contraction but without the diffuser to the same test section width with the diffuser (Figs. 23 and 24) shows why the addition of the diffuser did not increase the Mach number. The separated area appears the same in both cases and it can be assumed that the losses would be the same. A tremendous surging and buffeting of the main wind tunnel was experienced as the flow passed the heavily separated region of the diffuser. This phenomenon may have been captured in the lower picture in Fig. 24. Again as with the foils alone, with the increase of the foil test section, the separated region decreases until in Fig. 27, the foils mounted on the walls, very little separation is observed. This fact is confirmed by Table V.

No attempt was made to measure the Mach number of the smoke tunnel. As the same general type of flow was observed in the main wind tunnel at all Mach numbers, it was assumed that the smoke tunnel would give some

indication of the character of the flow regardless of the Mach number.

Summary of Results

A final summary of the experimental results is presented in Figs. 39(a), 39(b), and 39(c). An inspection of these figures shows that the 19 inch foil test section gives the highest Mach number. However, the superiority is not so great as to make that configuration clearly the best. Slight modifications in the foils could change the picture entirely. These figures do indicate that complete supplementary contractions within the main tunnel test section with appreciable contraction ratios actually give a Mach number decrease. It would seem that the width of the foil test section to be used would depend to a large extent on the width of the two-dimensional model to be tested. It appears definitely that within the limits of 12 to 24 inch foil test sections that approximately equal Mach numbers will be attained, with a slight advantage to a width somewhere between the two.

The results stated in this investigation are not final. Variations in foil geometry could result in results significantly different than those presented herein. A possible interesting variation would be to increase the contraction ratio by increasing the thickness of the foil. Interesting results should be obtained

by variation of the diffuser angle. A small vacuum pump might give enough suction to prevent separation in a diffuser of even larger half angle expansion than 16 degrees. This would offer possibilities of quite sizeable increases in Mach number.

CONCLUSIONS AND RECOMMENDATIONS

From the foregoing results it is concluded that:

1. The Mach number of a subsonic wind tunnel may be increased by suitably shaped foils that are readily installed or removed from the test section.
2. The magnitude of the increase depends upon the dimensions of the model to be tested.
3. The method of increase which offers the most promise is the mounting of foils vertically within the tunnel test section without a complete contraction and diffuser.
4. If the model to be tested is small compared to the original tunnel test section, the method of increase should be by means of vertically mounted foils and not by means of a smaller test section with a supplementary contraction and diffuser.
5. In this particular investigation the foils gave a Mach number increase of from .245 to .309, or an increase of 26.67 percent.

It is recommended that:

1. Further studies should be made to determine the optimum foil configuration for the largest Mach number increase.
2. A study be made on the use of suction through the foils to further increase the Mach number.

REFERENCES

Ref. 1: Hermann, Rudolf: Flow Characteristics of a Ram Inlet-Wind Tunnel Combination, Called The "Ram Tunnel", A Research Study for the Department of the Air Force, University of Minnesota, December 1954.

Ref. 2: Pope, Alan: Wind-Tunnel Testing, 1954, 2nd ed., John Wiley & Sons, Inc., New York.

Ref. 3: Pankhurst, R.C., and Holder, D.W.: Wind-Tunnel Technique, 1952, Sir Issaac Pitmen & Sons, Ltd., London.

Ref. 4: Patterson, G.N.: Modern Diffuser Design, Aircraft Engineering, Vol. X, Number 115, September 1938.

Ref. 5: Hermann, Rudolf: Supersonic Inlet Diffusers and Introduction to Internal Aerodynamics, 1956, Minneapolis-Honeywell Regulator Co., Minneapolis, Minnesota.

Ref. 6: Stanitz, John D.: Design of Two Dimensional Channels with Prescribed Velocity Distribution Along the Channel Walls. Solution by Greens Function, NACA TN 2595, January 1952.

Ref. 7: Cheers, F.: Notes on Wind Tunnel Contractions, Aeronautical Research Council Reports and Memorandum, 2137, 1945.

Ref. 8: Lighthill, M.J.: A New Method of Two Dimensional Aerodynamic Design, Aeronautical Research Council Reports and Memorandum, 2112, Appendices XIV to XVI, 1945.

Ref. 9: Stanitz, John D.: Design of Two Dimensional Channels with Prescribed Velocity Distribution Along the Channel Walls, Relaxation Solutions, NACA TN 2593, 1952.

Ref.10: Sheppard, J.J.Jr: The Barometer and the Manometer in Pressure Measurements, Rosemount Research Laboratories Engineering Memorandum No. 24, 1953.

Table I

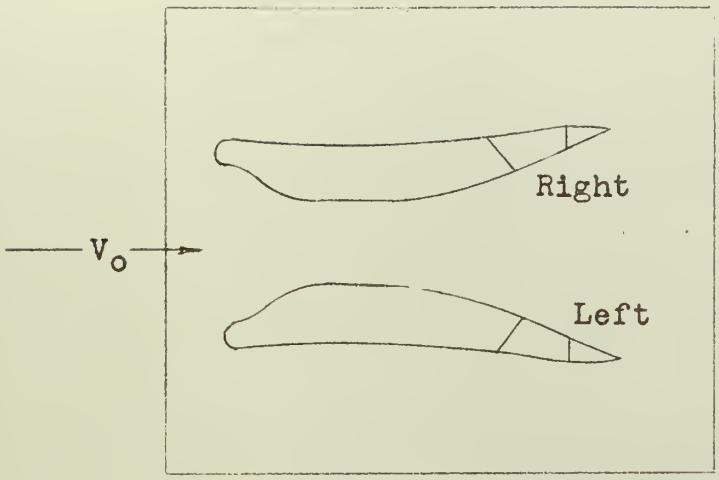

Total Pressure in Tunnel at:

V_o	Lbs/Ft^2 Gage
136	27.50
174	44.50
196	55.50

Pressure Points Shown in Fig. 3

Pressures shown as Lbs/Ft^2 gage

Left Foil

	Exterior				Interior			
V_o	Holes		Slots		Holes		Slots	
Ft/Sec	Total	Static	Total	Static	Total	Static	Total	Static
136	27.20	- 5.06	27.30	- 9.37	-10.11	-11.65	-13.89	-13.91
174	44.10	- 9.15	44.20	-15.89	-17.01	-17.81	-22.18	-21.98
196	54.60	-11.65	55.20	-20.42	-21.17	-22.10	-27.41	-27.00

Right Foil

	Exterior				Interior			
V_o	Holes		Slots		Holes		Slots	
Ft/Sec	Total	Static	Total	Static	Total	Static	Total	Static
136	27.72	2.44	27.90	.55	27.50	-16.91	26.85	- 2.45
174	44.10	3.98	44.60	.83	44.30	-27.10	42.80	- 3.44
196	55.00	5.06	55.60	.83	55.15	-33.81	54.10	- 4.27

Table II

Right Foil

Velocities and Mach Numbers at Trailing Edge, Exterior and Interior

Exterior			Interior	
V_o Ft/Sec	V Ft/Sec	M-No.	V Ft/Sec	M-No.
136	152	.134	152	.135
174	193	.169	194	.170
196	218	.190	219	.191

Right Foil

Pressures Across Trailing Edge Lbs/Ft^2 Gage

Exterior			Interior	
V_o Ft/Sec	Total	Static	Total	Static
136	27.62	+1.24	26.78	+.24
174	43.75	1.99	42.75	.41
196	55.00	2.32	53.75	.46

Table III

Velocities and Mach Numbers Under Various Conditions of Holes and Slots Open

V_1 Velocity in Foil Test Section

M_1 Mach Number in Foil Test Section

12 Inch Foil Test Section

V_o Ft/Sec	Holes and Slots Closed		Holes Closed Slots Open	
	V_1	M_1	V_1	M_1
105	185	.164	182	.160
136	242	.213	239	.211
150	266	.235	263	.232
163	286	.252	285	.251
174	307	.270	302	.267
186	327	.287	323	.285
196	348	.304	337	.297

Holes Open Slots Closed

V_o Ft/Sec	V_1	M_1
105	182	.163
136	240	.211
150	266	.235
163	289	.255
174	312	.274
186	330	.291
196	350	.306

Table III (Cont'd.)

19 Inch Foil Test Section

V_o Ft/Sec	Holes and Slots Closed		Holes Closed Slots Open	
	V_1	M_1	V_1	M_1
105	168	.149	168	.148
136	222	.195	222	.196
150	244	.216	245	.216
163	266	.235	264	.232
174	285	.251	284	.250
186	304	.267	304	.269
196	321	.281	321	.280
216	355	.309	352	.308

24 Inch Foil Test Section

V_o Ft/Sec	Holes and Slots Closed		Holes Closed Slots Open	
	V_1	M_1	V_1	M_1
105	158	.141	158	.140
136	206	.182	203	.181
150	228	.201	226	.200
163	248	.218	245	.216
174	266	.234	264	.232
186	282	.248	282	.247
196	300	.262	299	.261
216	334	.291	331	.288
225	348	.302	346	.300

Table IV

Percent Increase of Velocity and Mach Number Over That Given by Incompressible Theory

12 Inch Foil Test Section

V_o 105 Ft/Sec		V_o 196 Ft/Sec		Mean	
V	M	V	M	V	M
6.9%	7.2%	8.4%	8.6%	7.6%	7.9%

19 Inch Foil Test Section

V_o 105 Ft/Sec		V_o 196 Ft/Sec		Mean	
V	M	V	M	V	M
13.5%	13.8%	18.3%	17.9%	15.9%	15.9%

24 Inch Foil Test Section

V_o 105 Ft/Sec		V_o 196 Ft/Sec		Mean	
V	M	V	M	V	M
14.5%	15.8%	17.6%	17.5%	16.0%	16.7%

Table V

Data on Flow Through Complete Contractions

	12"T.S.	19"T.S.	24"T.S.	12"T.S. No Diffuser	39.3"T.S. (Foils on wall)
V_o Max.	49	73	100	49	258
V_1	209	204	217	208	344
M_1	.184	.180	.191	.183	.299

Test Section

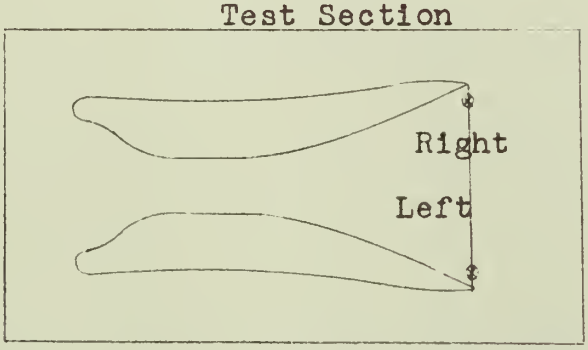

All Pressures Lbs/Ft^2 Gage

12 Inch T.S. Total Pressure No Losses 26.31				19 Inch T.S. Total Pressure No Losses 28.9			
Left Foil		Right Foil		Left Foil		Right Foil	
Total	Static	Total	Static	Total	Static	Total	Static
12.56	-5.80	26.02	-1.86	20.50	-5.18	28.80	-1.12

24 Inch T.S. Total Pressure No Losses 33.20				39.3 Inch T.S. (Foils on Wall) Total Pressure No Losses 64.5			
Left Foil		Right Foil		Left Foil		Right Foil	
Total	Static	Total	Static	Total	Static	Total	Static
32.06	-3.31	33.10	-2.49	64.50	-8.29	64.40	-12.47

Table VI

Velocities and Mach Numbers Ahead of the Foils

Showing the Contraction of the Streamlines

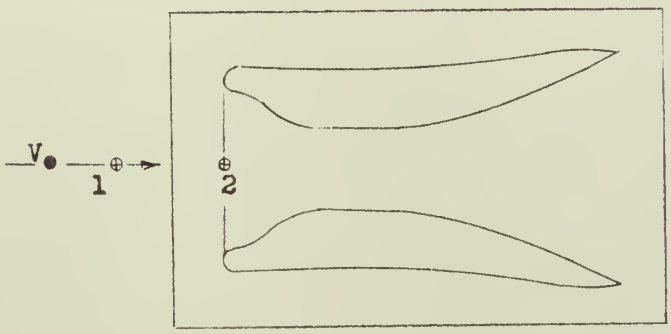

12 Inch Foil Test Section

1		2	
V_1 Ft/Sec	M_1	V_2 Ft/Sec	M_2
136	.121	167	.148
174	.152	212	.186
196	.170	239	.208

19 Inch Foil Test Section

1		2	
V_1 Ft/Sec	M_1	V_2 Ft/Sec	M_2
136	.121	177	.154
174	.152	227	.199
196	.170	254	.221

24 Inch Foil Test Section

1		2	
V_1 Ft/Sec	M_1	V_2 Ft/Sec	M_2
136	.121	173	.153
174	.152	221	.194
196	.170	249	.217

Table VII

Comparison of Theoretical and Experimental Results

Test Section

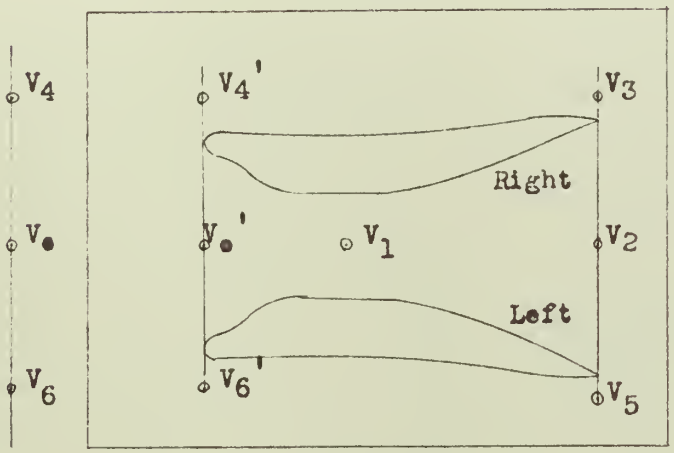

All Velocities Ft/Sec

Right

	V_2	V_3			V_4'			V_o	
V_o	Exp. Integrated Velocities	Exp.	Calc.	% Er.	Exp.	Calc.	% Er.	Calc.	% Er.
136	114	152	153	.66%	128	124	3.1%	134	1.5%
174	145	193	193	0	160	157	1.9%	170	2.3%
195	157	218	218	0	180	177	1.6%	189	3.6%

	V_4			V_1			V_o'		
V_o	Exp.	Calc.	% Er.	Exp.	Calc.	% Er.	Exp.	Calc.	% Er.
136	132	134	1.5%	239	249	4.2%	167	152	9.0%
174	168	170	1.2%	310	317	2.2%	212	193	9.0%
196	188	189	.5%	348	343	1.4%	239	209	12.5%

Left

	V_5			V_6'			V_6			V_o	
V_o	Exp.	Calc.	% Er.	Exp.	Calc.	% Er.	Exp.	Calc.	% Er.	Calc.	% Er.
136	175	180	2.8%	139	146	5.0%	137	148	8.0%	148	8.8%
174	223	231	3.6%	179	187	4.5%	175	189	8.0%	189	8.6%
196	252	260	3.1%	205	210	2.4%	197	210	6.6%	210	7.1%

Fig. 1

Pitot Tube

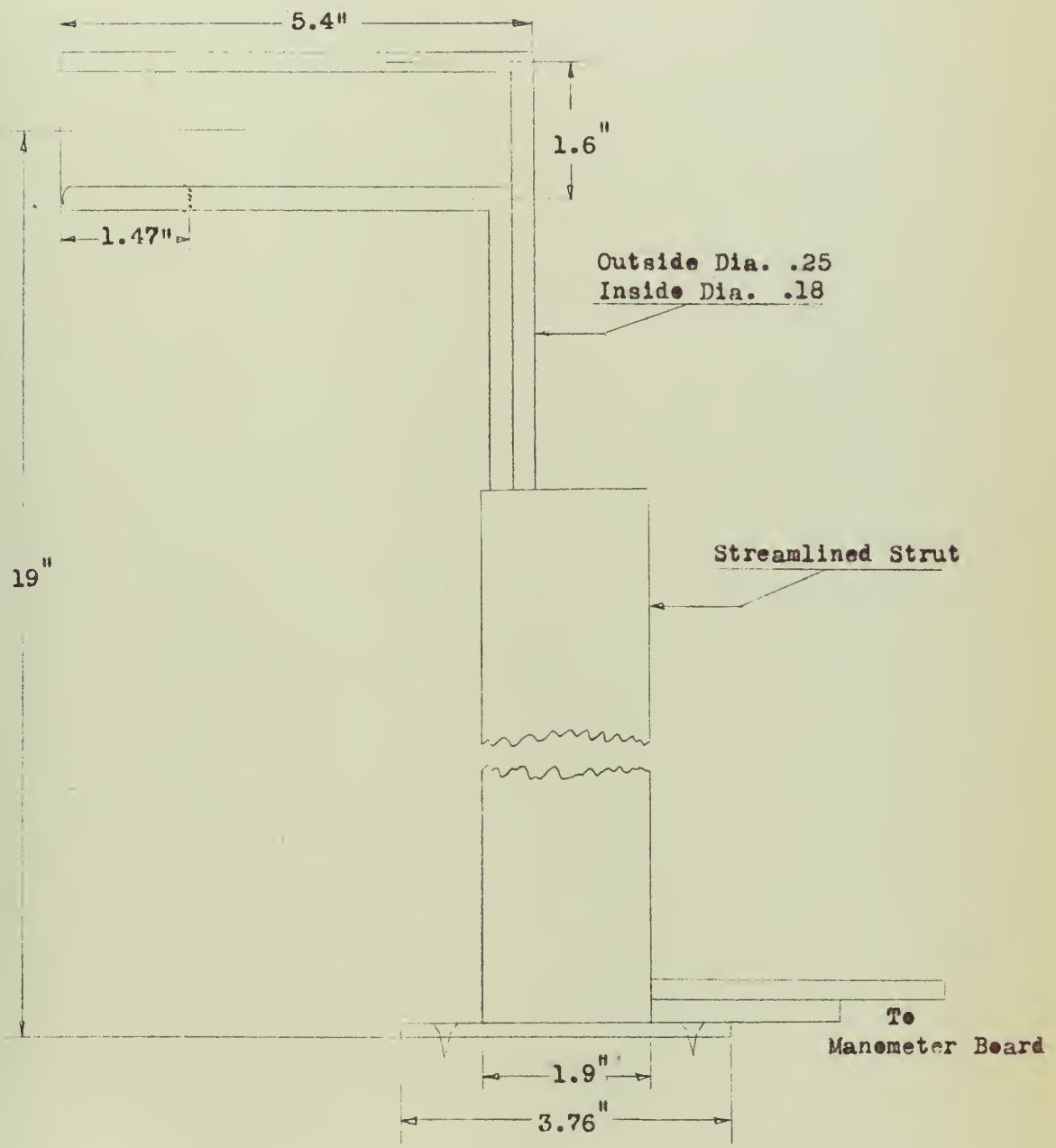

Scale 2:1

Fig. 2

Foil

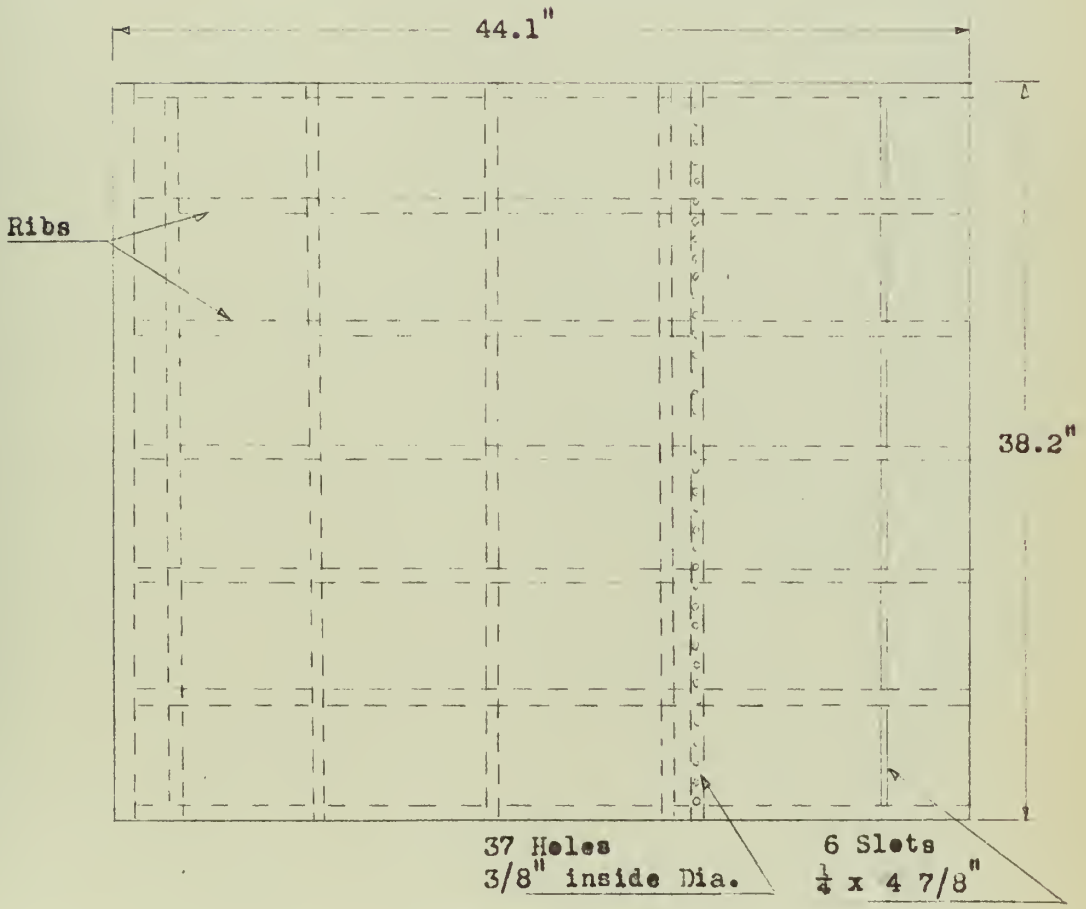

Scale 10:1

Fig. 3

Foil Tunnel Installation and
Pressure Points
12 inch Test Section

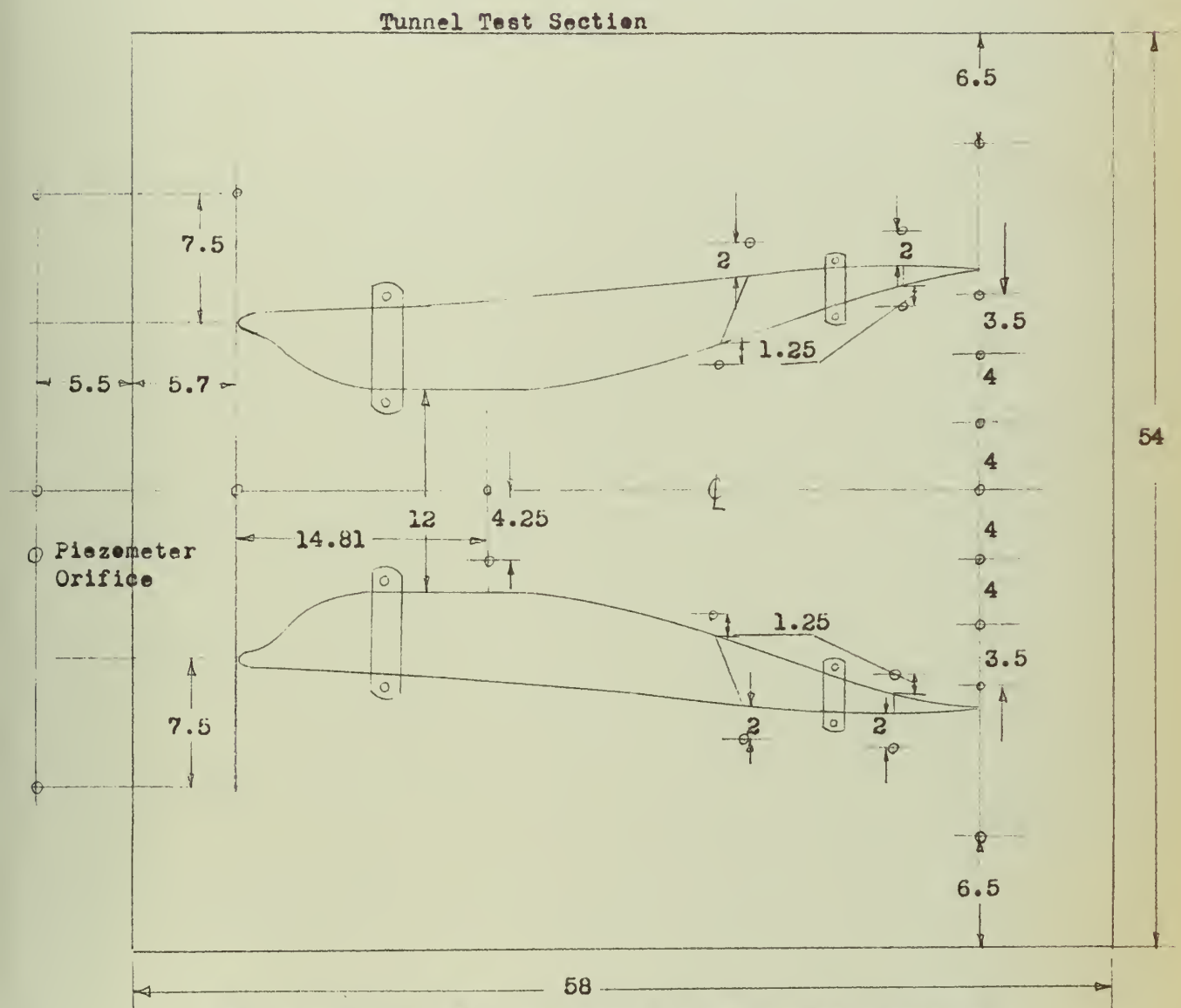

⊙ Points at which total and static pressures were measured

All measurements in inches

Scale 10:1

Fig. 4

Foil Tunnel Installation and
Pressure Points
19 inch Test Section

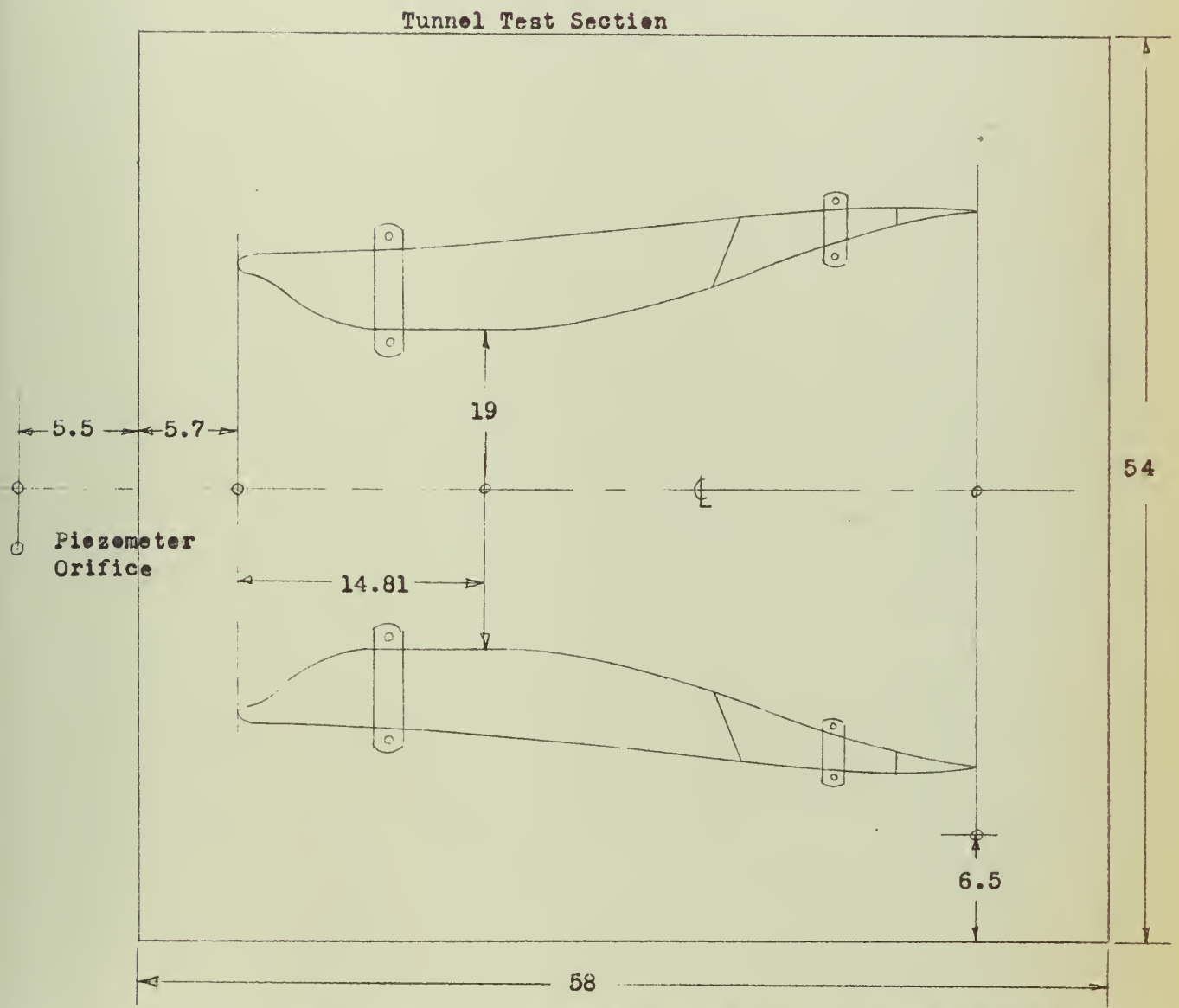

⊙ Points at which total and static pressures were measured
All measurements in inches
Scale 10:1

Fig. 5

Foil Tunnel Installation and
Pressure Points
24 inch Test Section

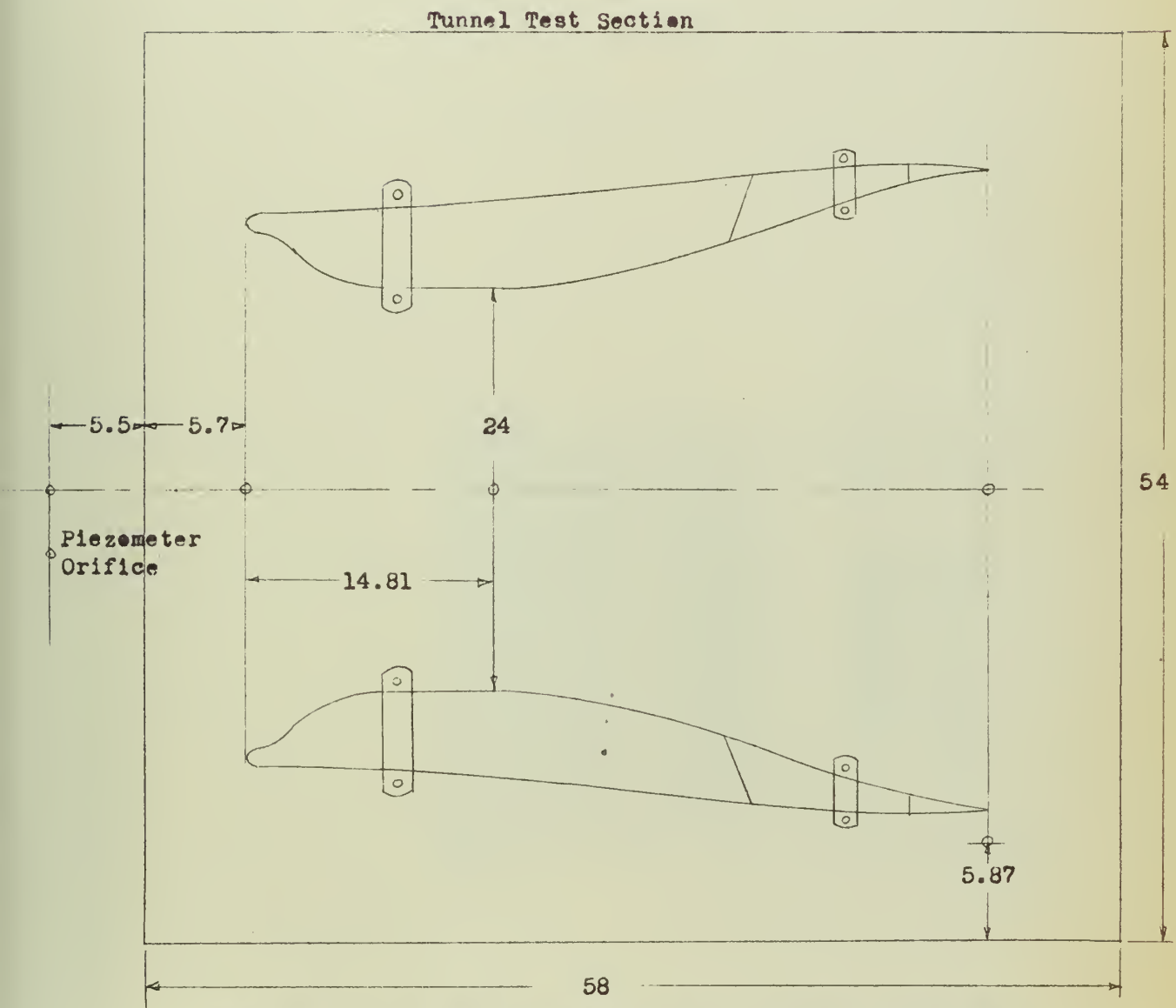

Points at which total and static pressures were measured
All measurements in inches
Scale 10:1

Page

Fall Installation

Looking downstream from southeast end

of Mile

FIG. 7

CONTRACTION AND DIFFUSER INSTALLATION AND PRESSURE POINTS .

12 INCH TEST SECTION

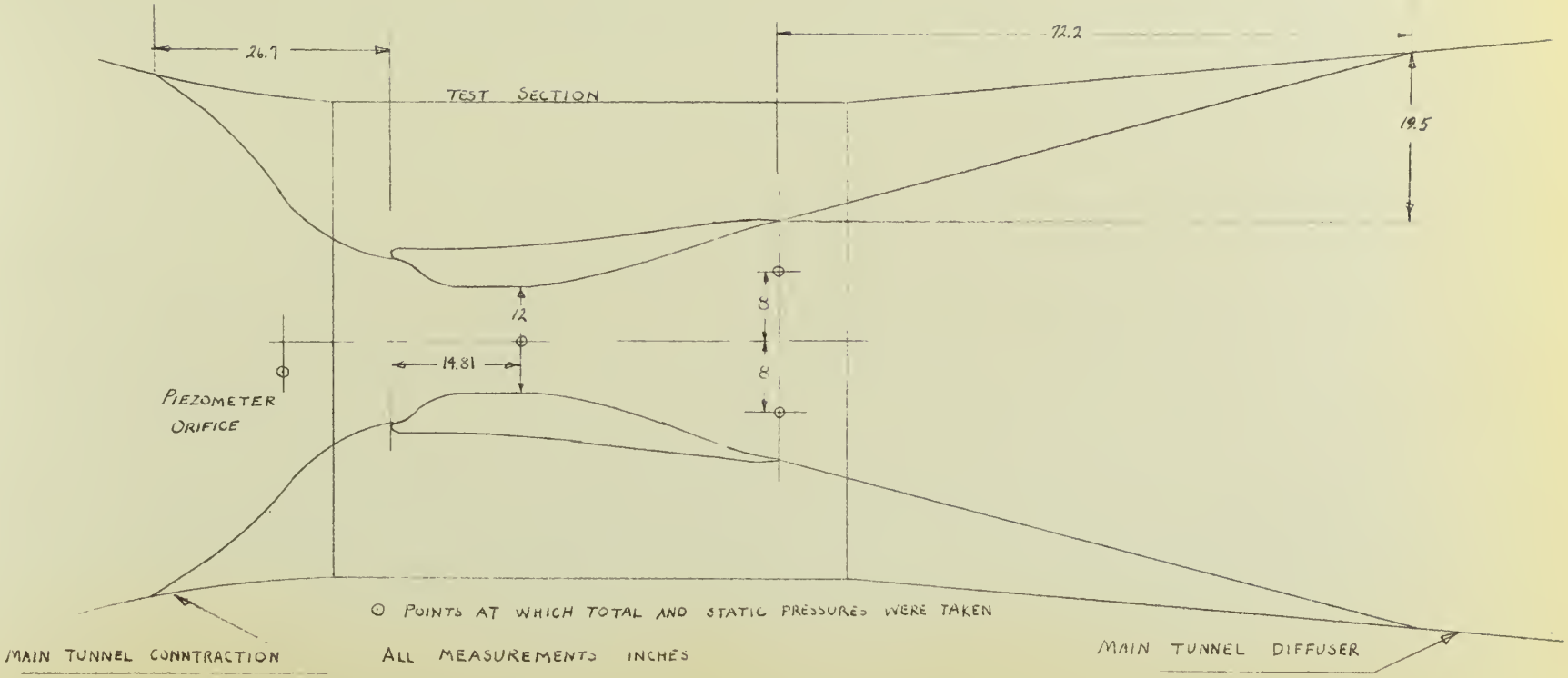

⊙ POINTS AT WHICH TOTAL AND STATIC PRESSURES WERE TAKEN

ALL MEASUREMENTS INCHES

SCALE 20:1

Contraction and Diffuser Installation and Pressure Points 19 inch Test Section

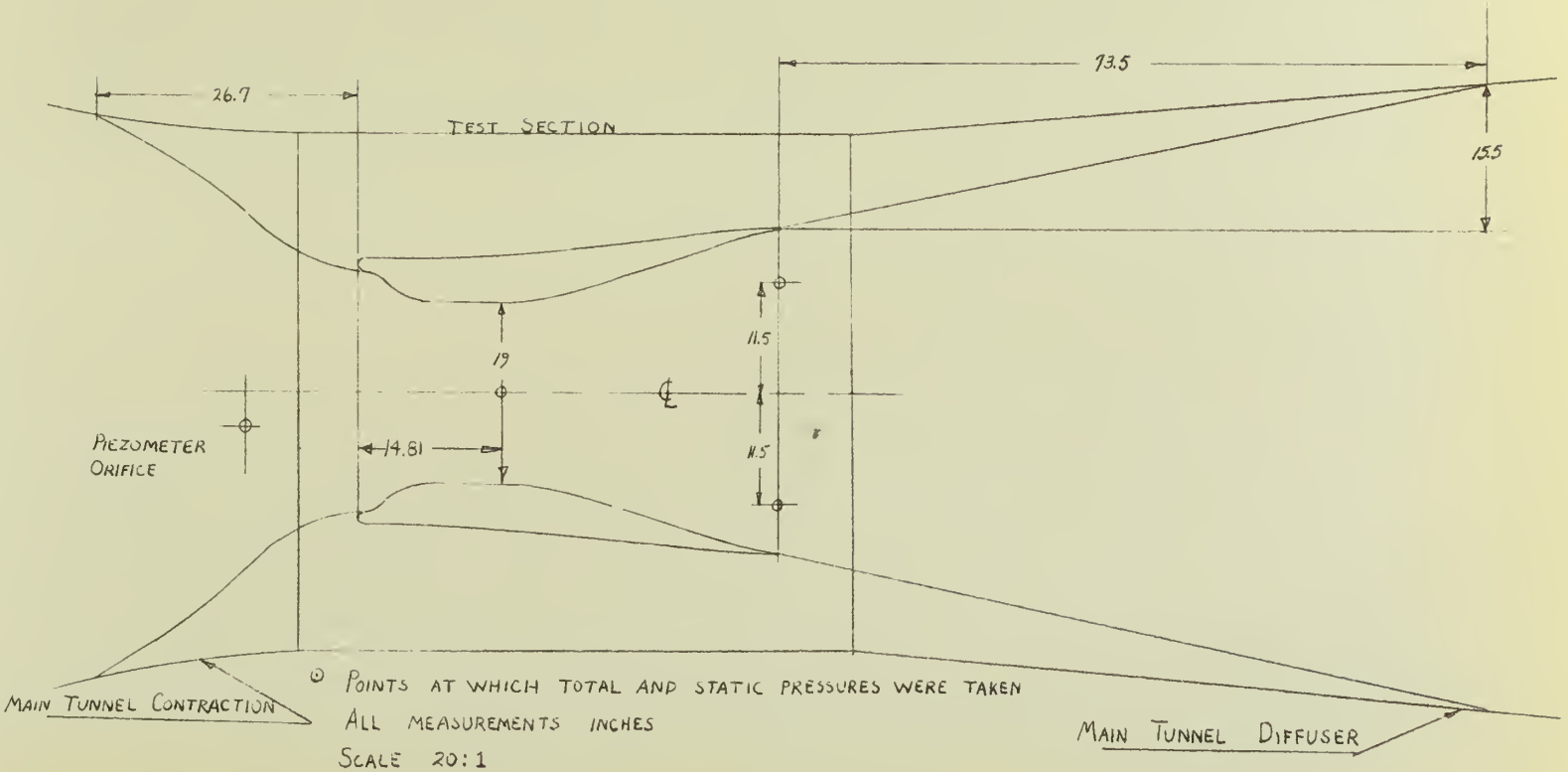

⊙ Points at which total and static pressures were taken

All measurements inches

Scale 20:1

FIG. 9

CONTRACTION AND DIFFUSER INSTALLATION
AND PRESSURE POINTS
24 INCH TEST SECTION

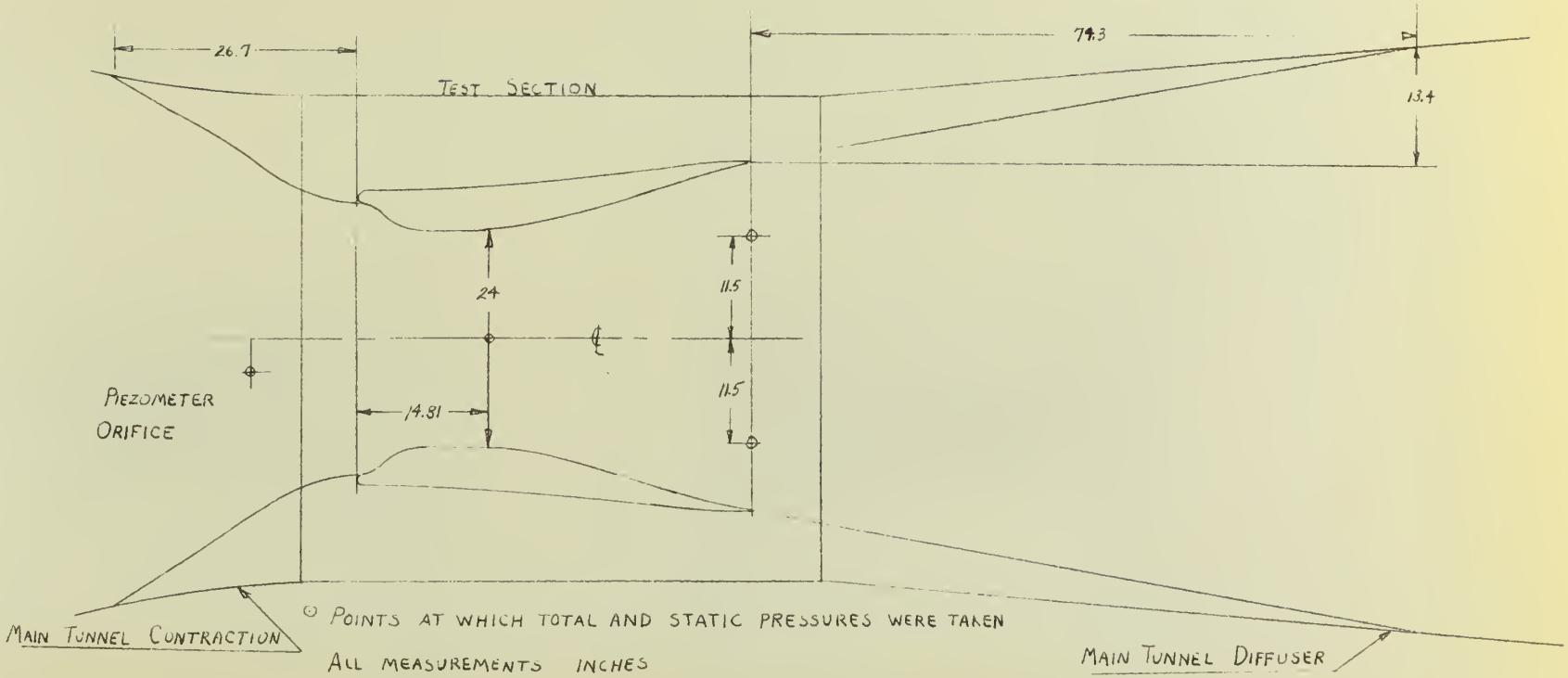

Fig. 20

Contraction and Diffuser Installation

Contraction Looking Downstream

Fig. 11

Foils Mounted on Wall and
Pressure Points

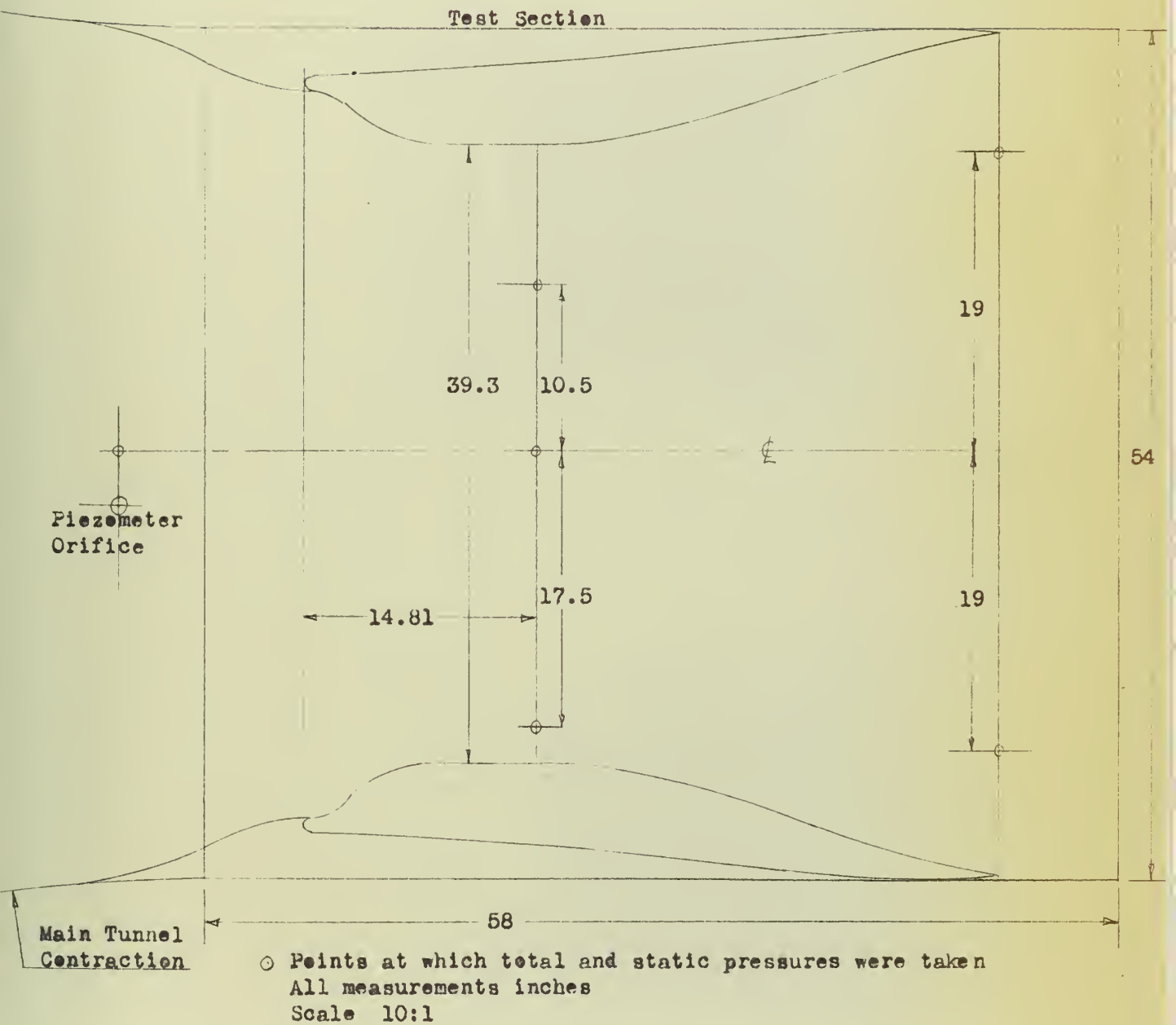

⊙ Points at which total and static pressures were taken
All measurements inches
Scale 10:1

Fig. 2

Test Sections as Test Series (cont.)

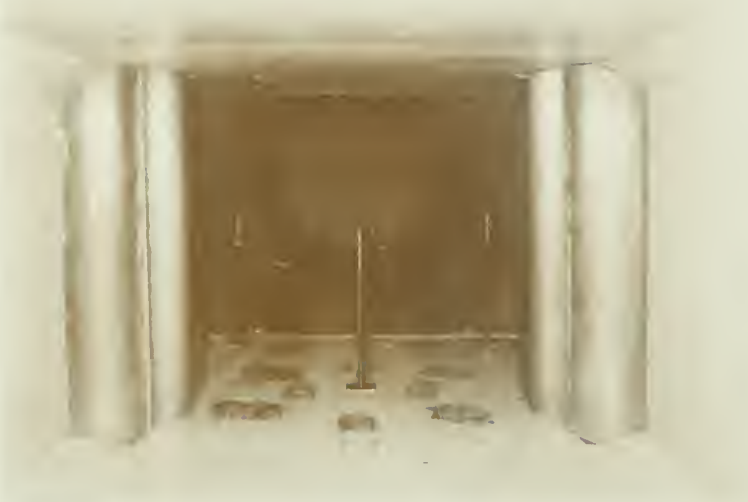

Contraction Looking Downstream

Diffuser Looking Upstream

Fig. 13

Schematic of Smoke Tunnel

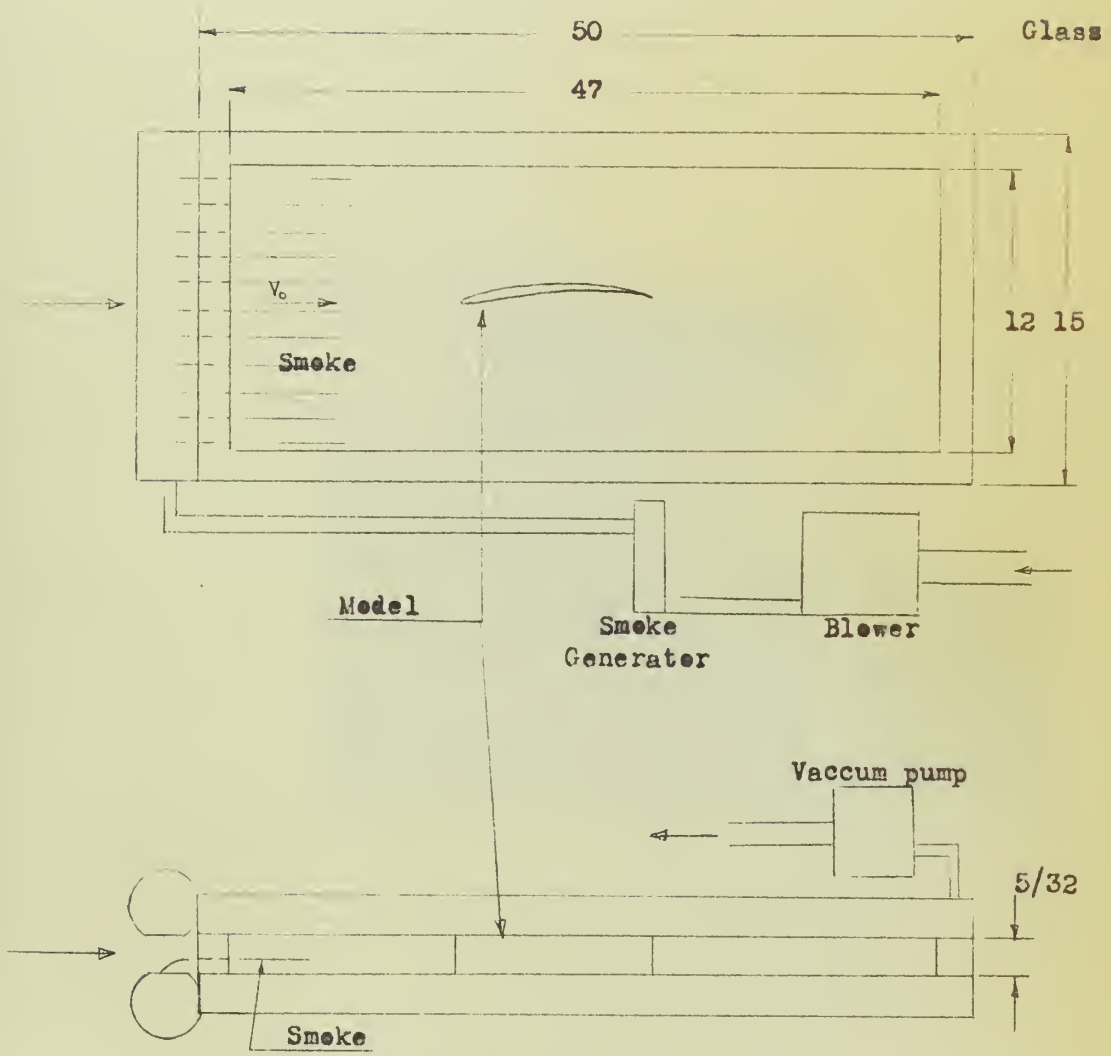

All Measurements inches

Fig. 11

Smoke Tunnel

Fig. 15

Tuft Photographs with Foil
Mounted Near Wall

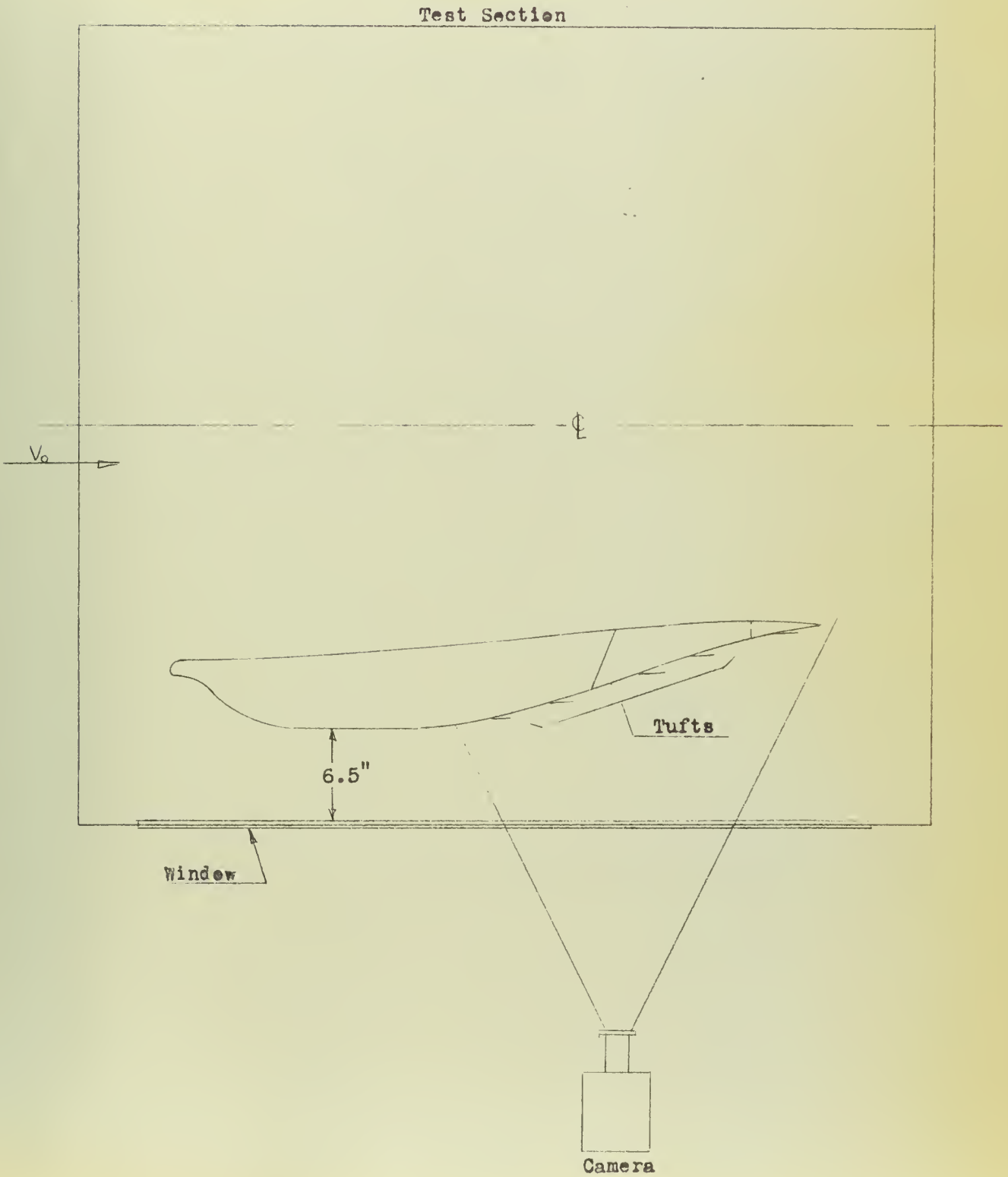

Fig. 16

Tuft Photographs with Foil
Mounted in Normal Position

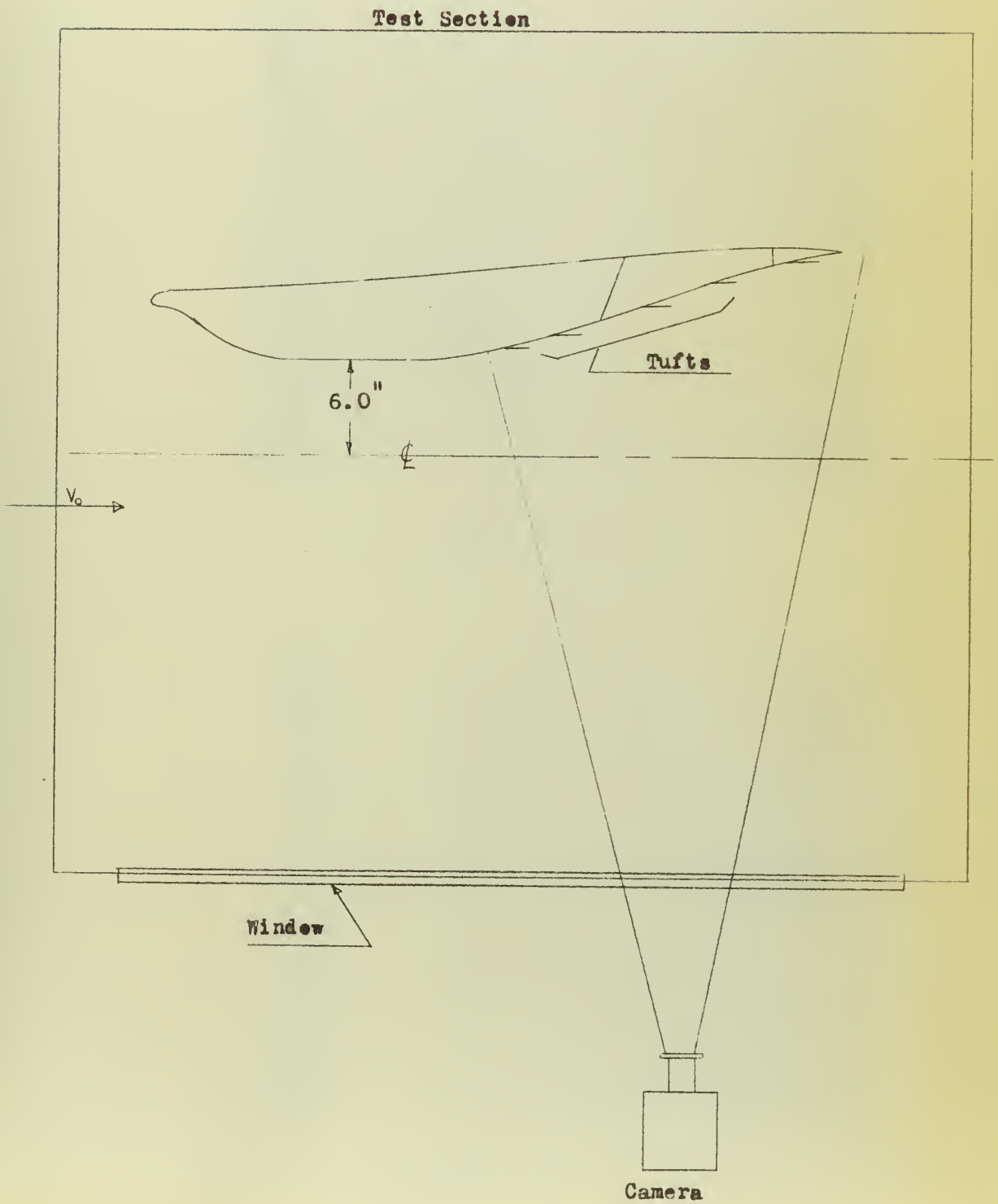

Fig. 17

Tuft Photographs-Foil Mounted Near Trail

Flow From Left to Right

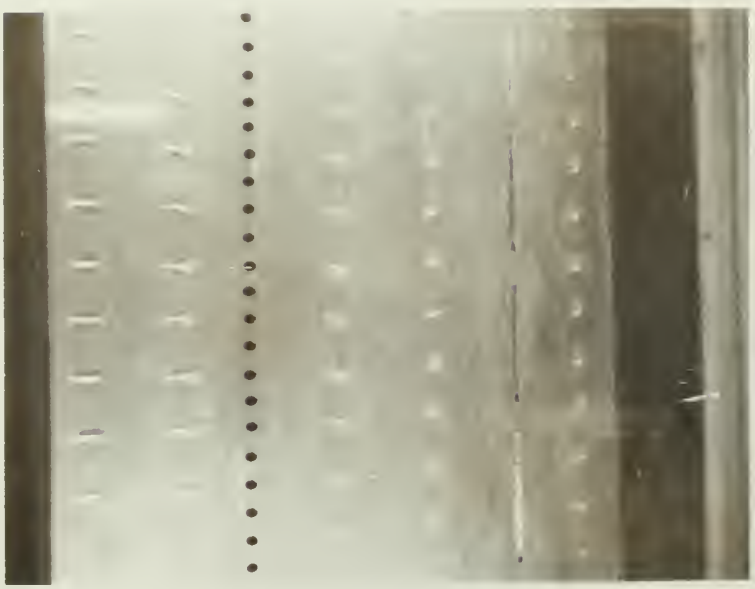

Holes and Slots Open

Holes and Slots Closed

Fig. 16

Tuft Photographs-Tail Mounted in Normal Position

Flow from Left to Right

Holes and Slots Open

Holes and Slots Closed

Fig. 19

Calibration of Main Tunnel Test Section

⊙ Pitot Tube Measurements

⊡ Piezometer Measurements

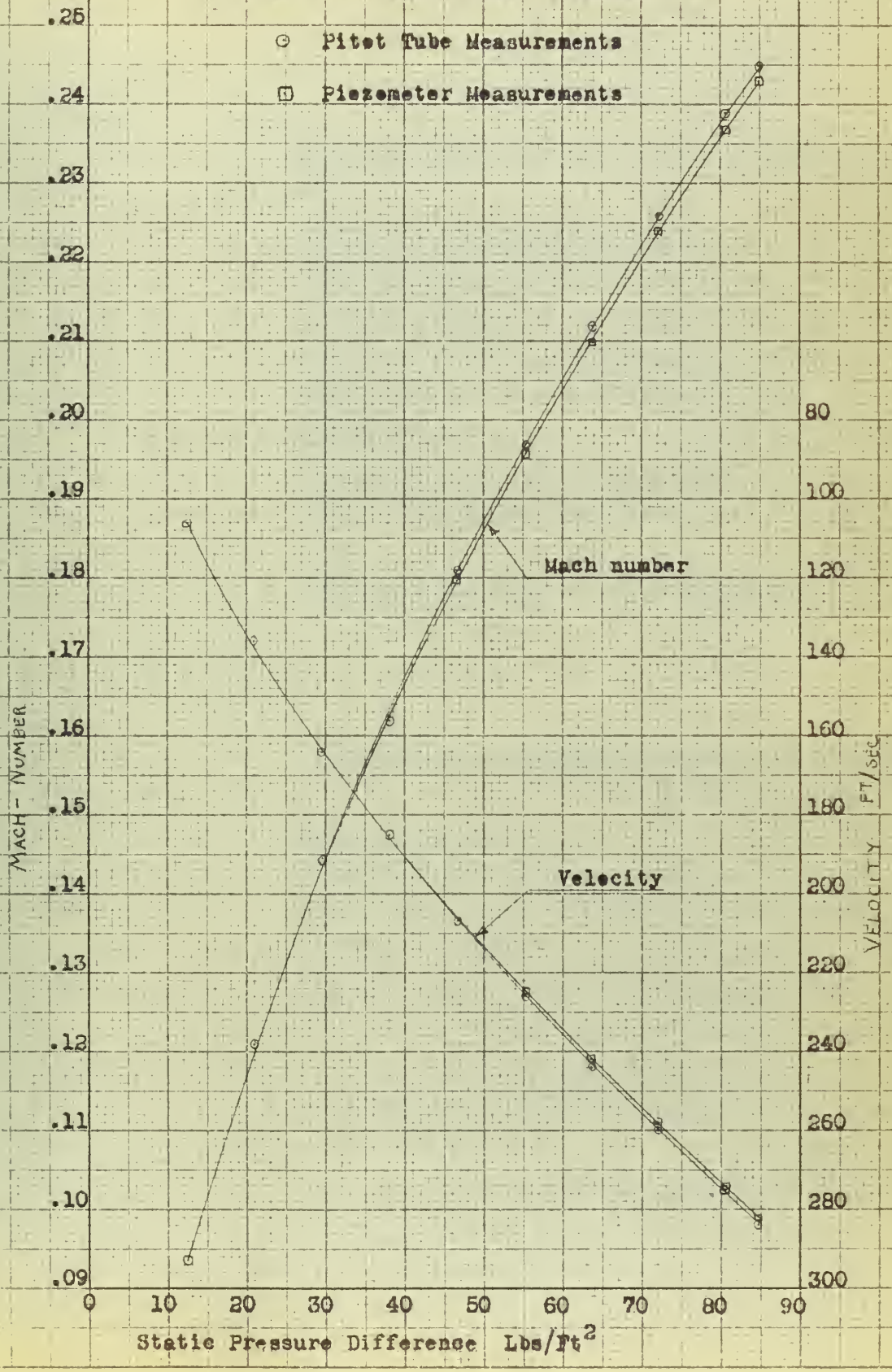

Fig. 20

Smoke Tunnel

Foils Alone

12 Inch Foil Test Section

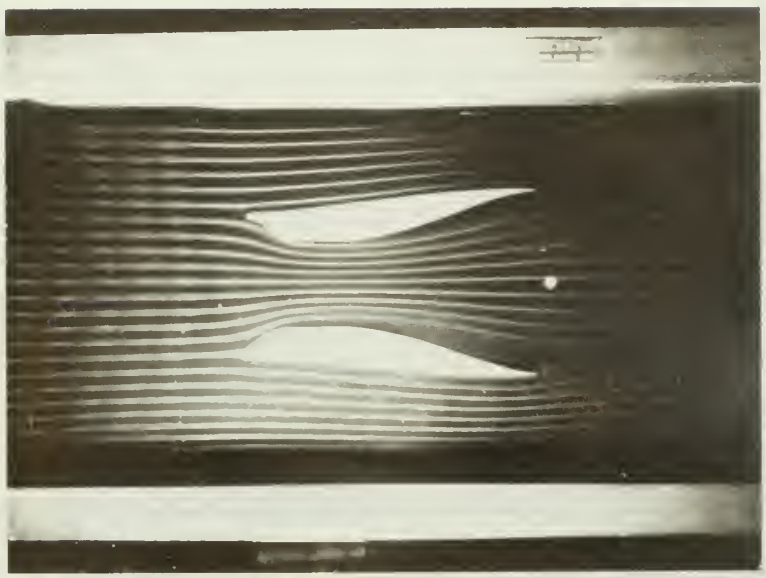

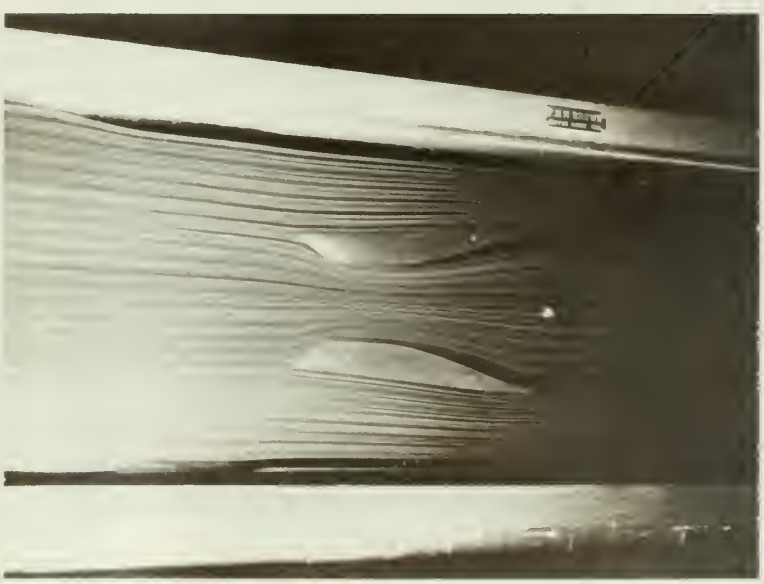

Fig. 21

Smoke Tunnel

Foils Alone

19 Inch Foil Test Section

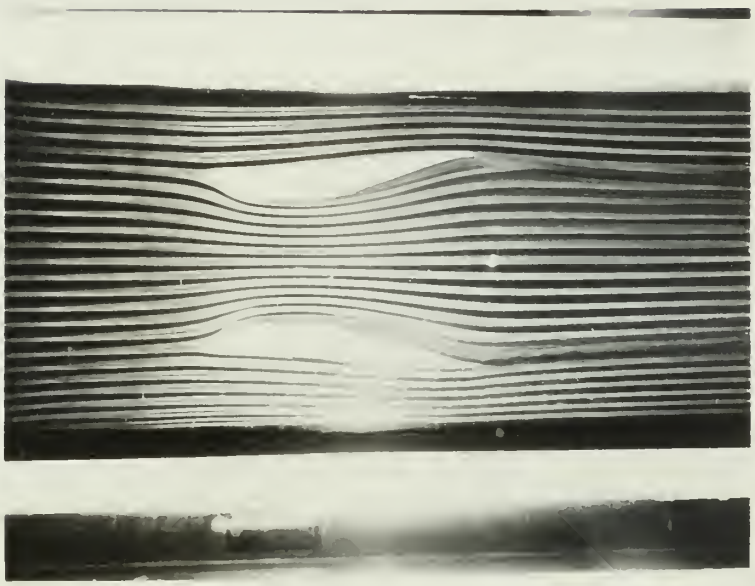

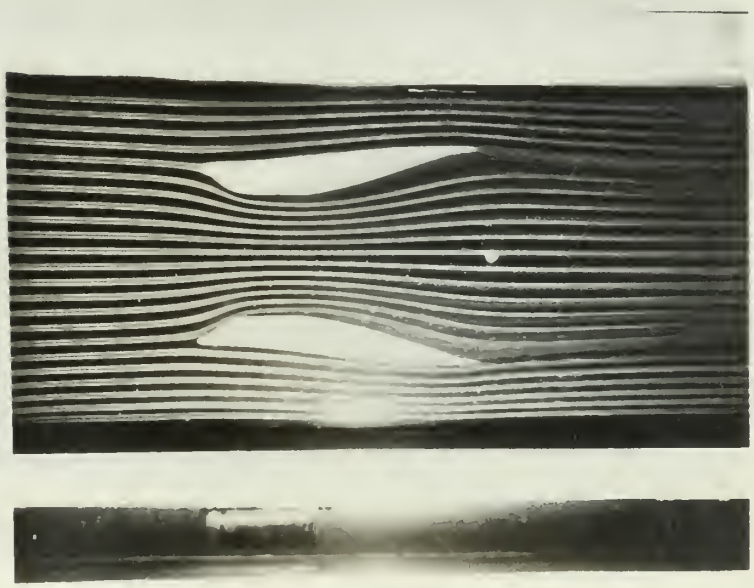

Fig. 22

Smoke Tunnel

Foils Alone

24 Inch Foil Test Section

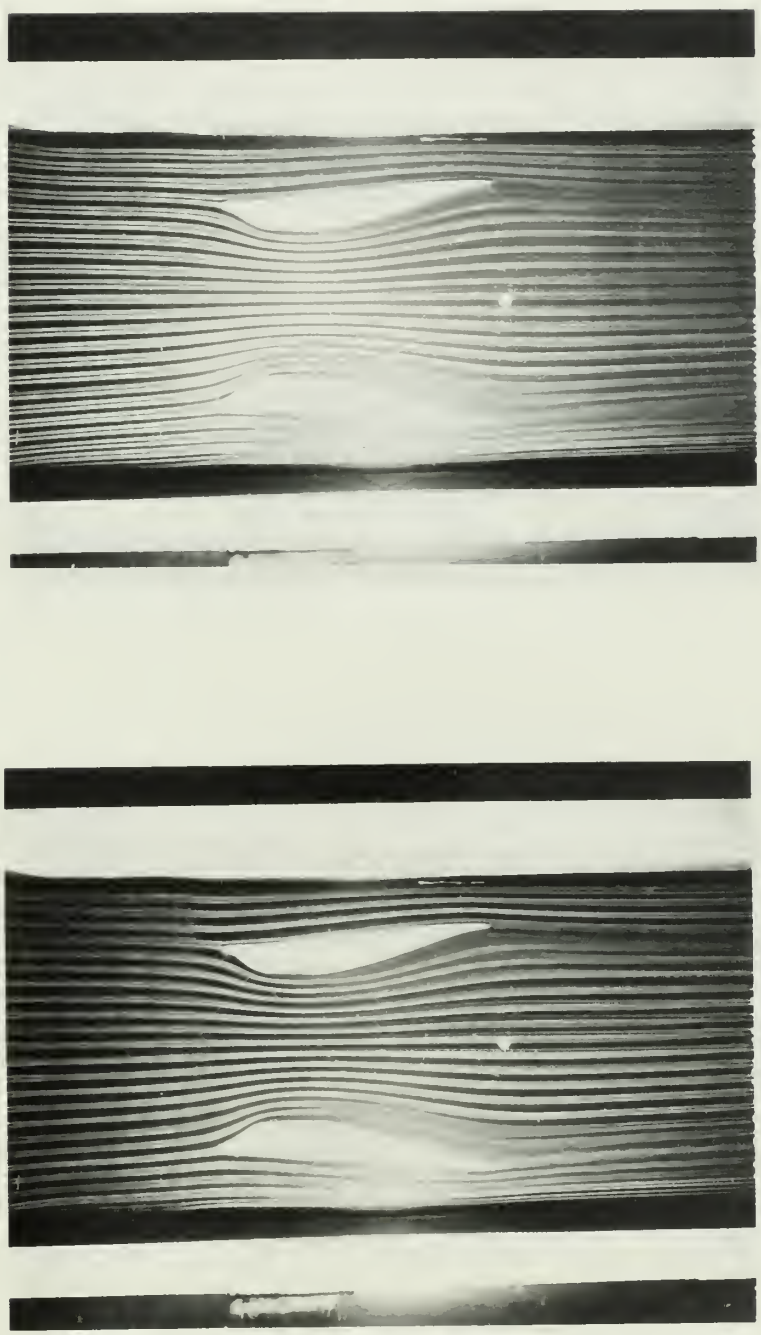

Fig. 23

Smoke Tunnel

Foils With Contraction

12 Inch Foil Test Section

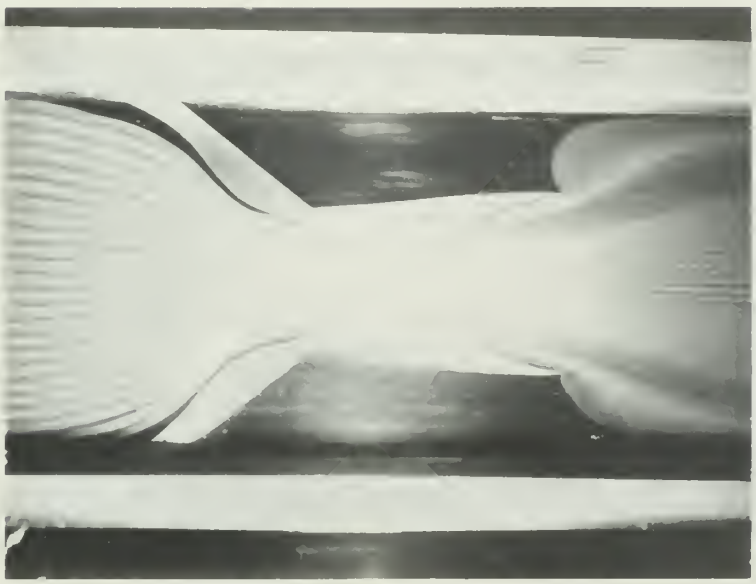

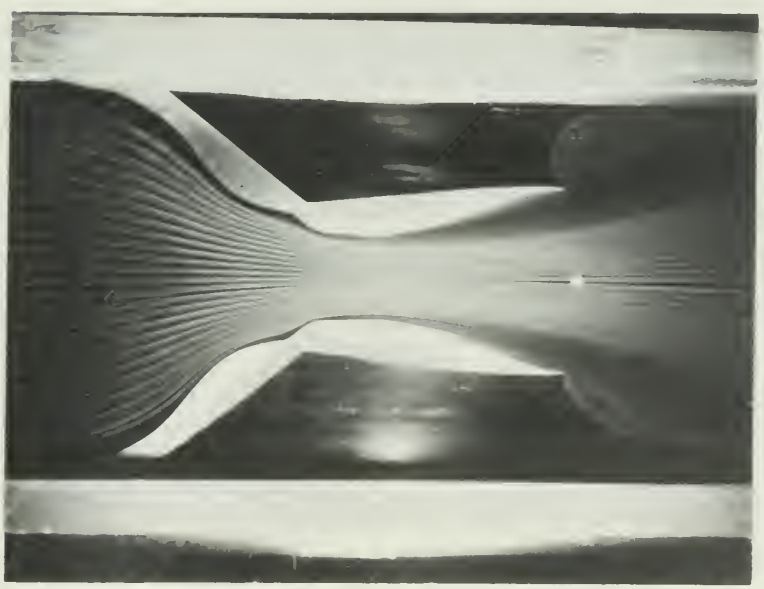

Fig. 24

Smoke Tunnel

Foils With Contraction And Diffuser

12 Inch Foil Test Section

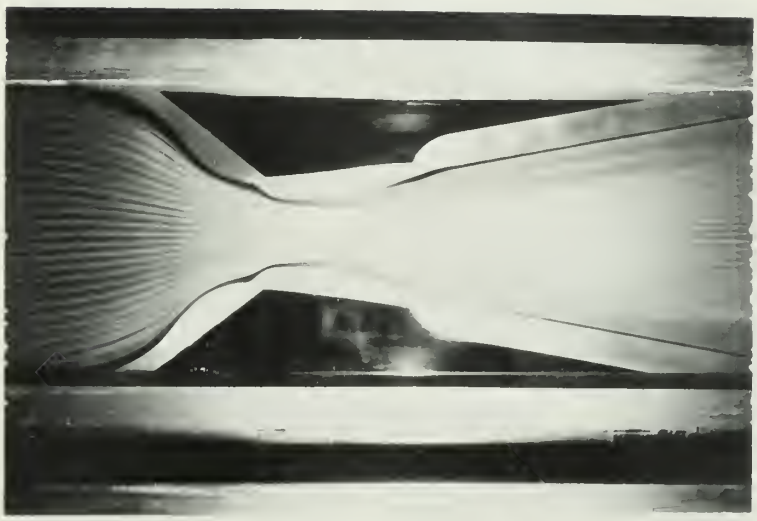

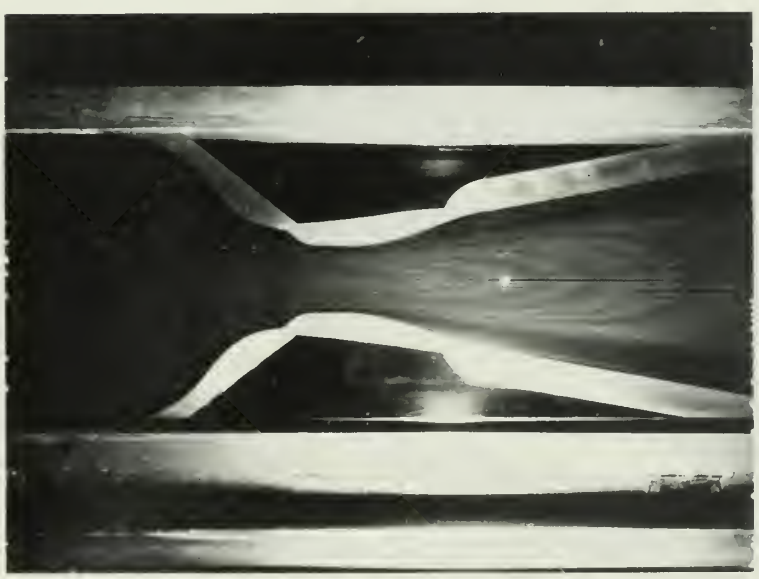

Fig. 25

Smoke Tunnel

Foils With Contraction And Diffuser

19 Inch Test Section

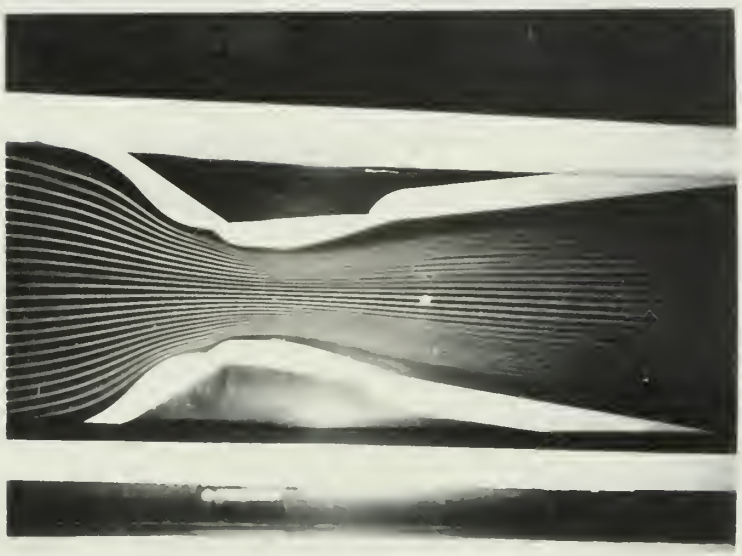

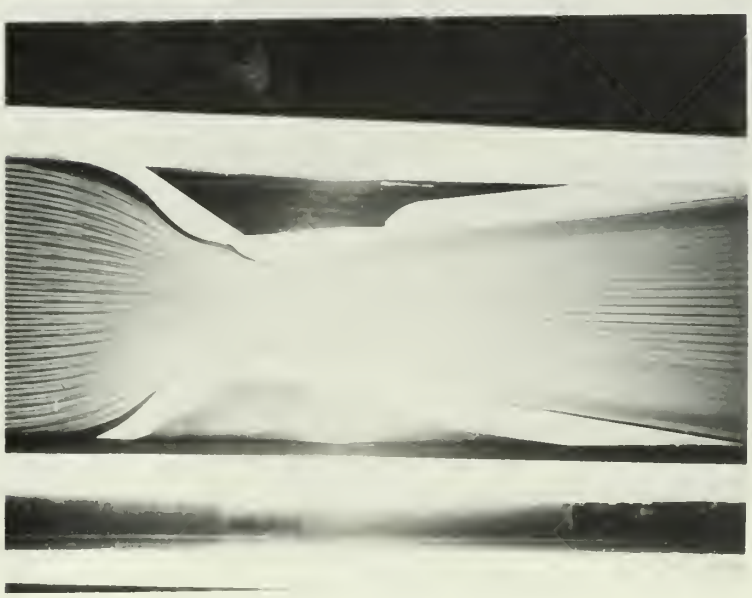

Fig. 26

Smoke Tunnel

Foils With Contraction And Diffuser

24 Inch Foil Test Section

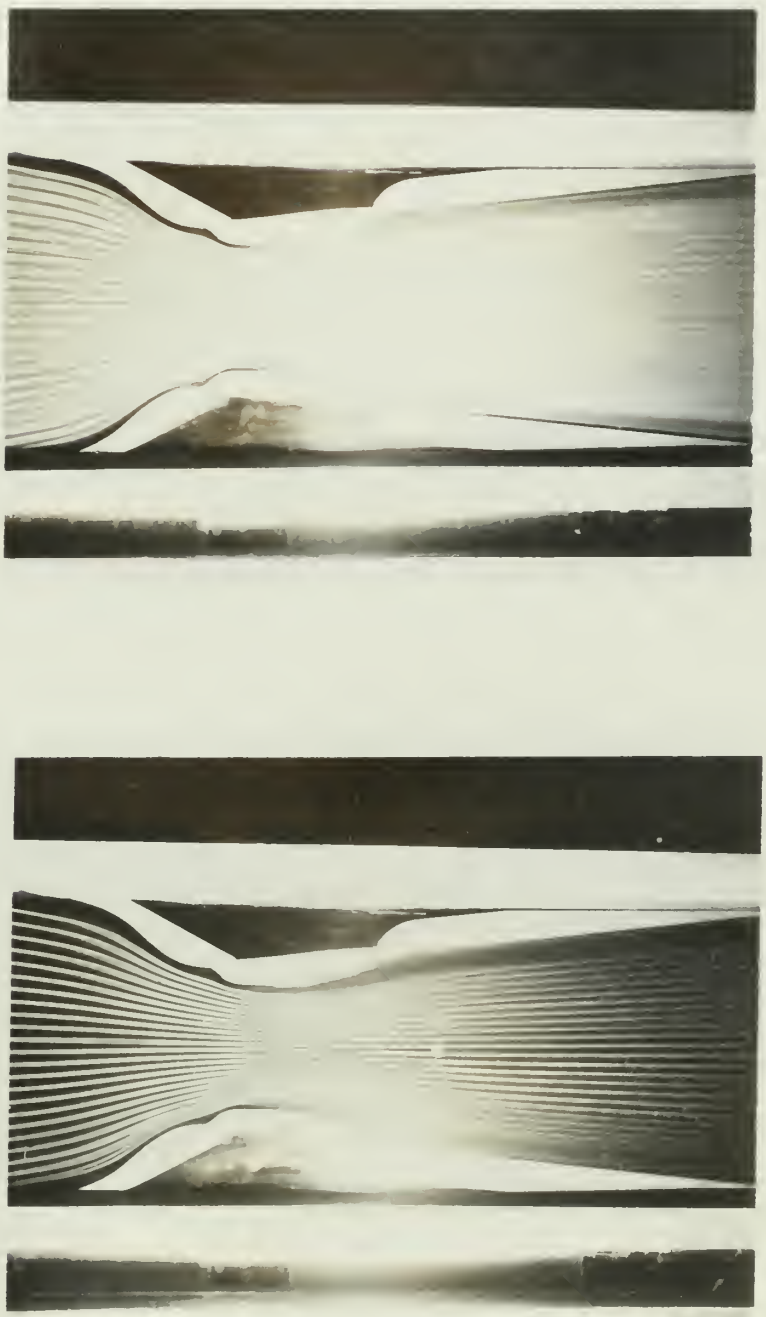

Fig. 27

Smoke Tunnel

Foils Mounted on Tunnel Walls

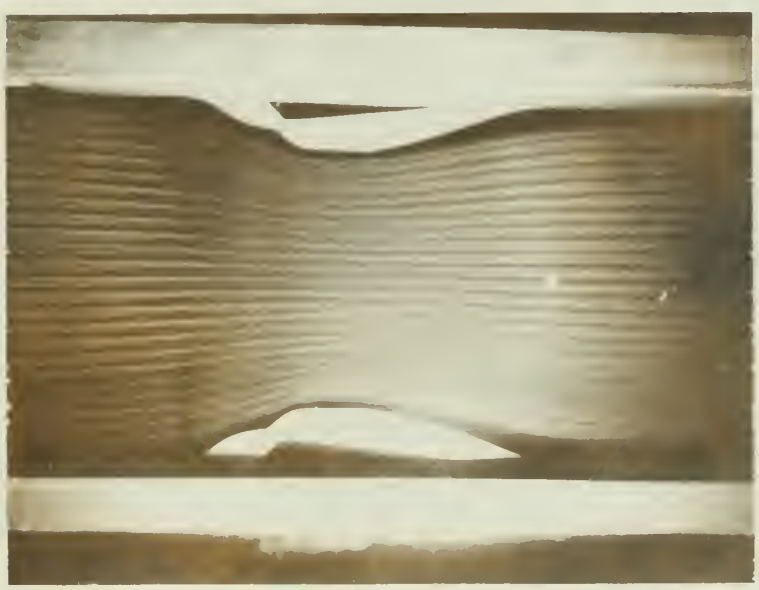

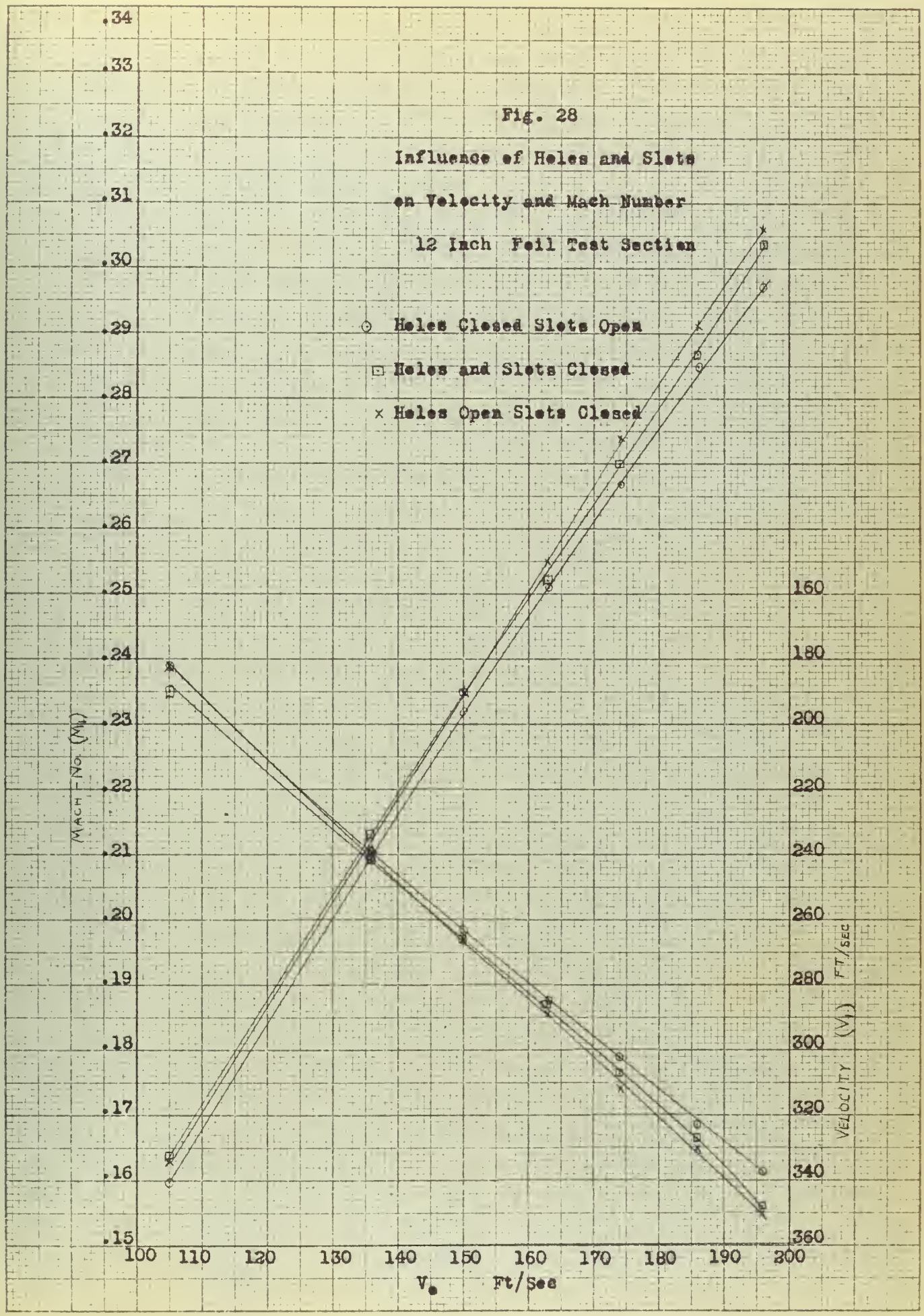
Fig. 28
Influence of Holes and Slots
on Velocity and Mach Number
12 Inch Foil Test Section
⊙ Holes Closed Slots Open
⊡ Holes and Slots Closed
× Holes Open Slots Closed
MACH No. (M1)
VELOCITY (V1) FT/SEC
V∞ Ft/Sec
.34
.33
.32
.31
.30
.29
.28
.27
.26
.25
.24
.23
.22
.21
.20
.19
.18
.17
.16
.15
160
180
200
220
240
260
280
300
320
340
360
100
110
120
130
140
150
160
170
180
190
200

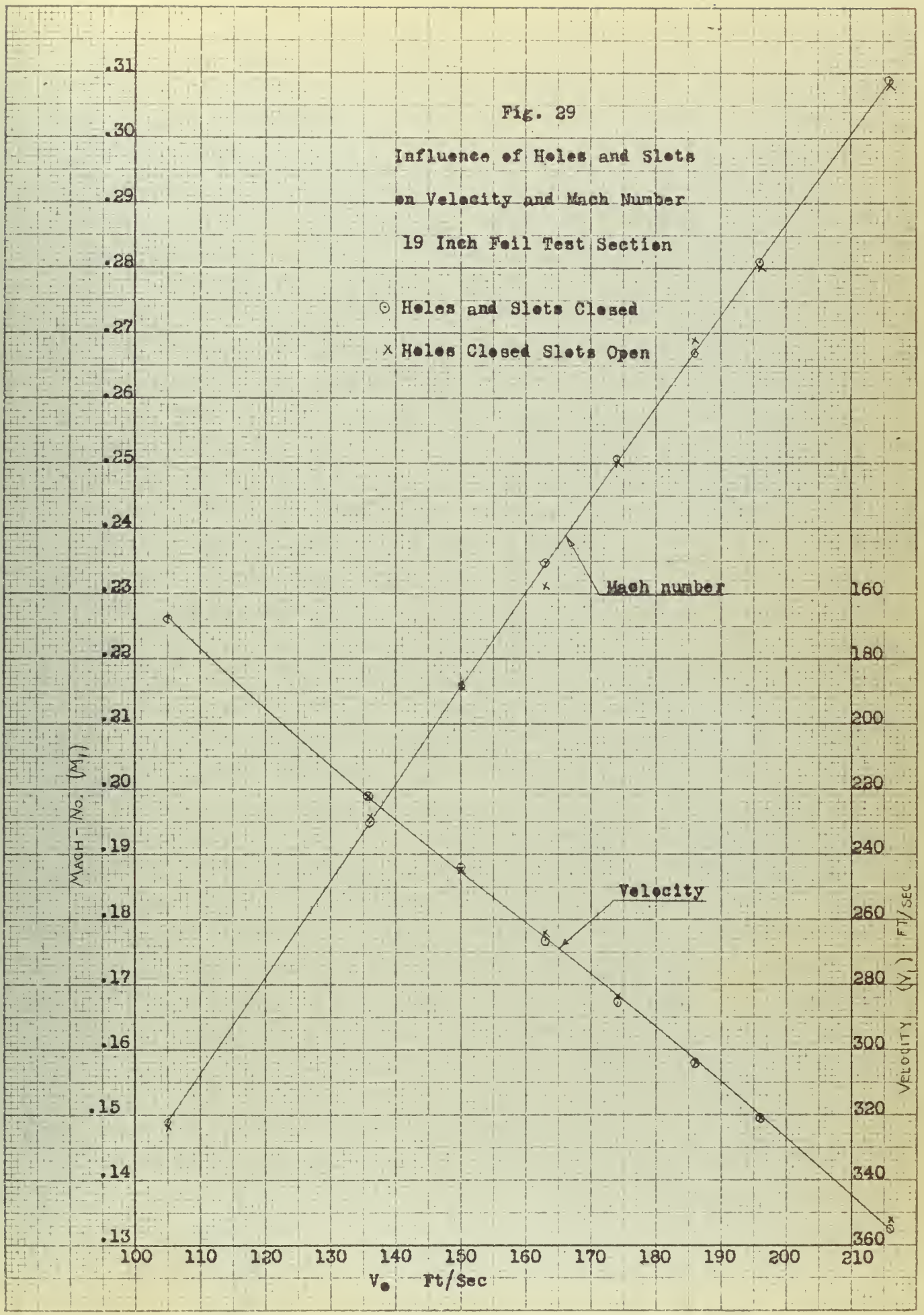
Fig. 29
Influence of Holes and Slots
on Velocity and Mach Number
19 Inch Foil Test Section
⊙ Holes and Slots Closed
x Holes Closed Slots Open
Mach number
Velocity
MACH - No. (M1)
VELOCITY (V1) FT/SEC
Vo Ft/Sec
.31
.30
.29
.28
.27
.26
.25
.24
.23
.22
.21
.20
.19
.18
.17
.16
.15
.14
.13
160
180
200
220
240
260
280
300
320
340
360
100
110
120
130
140
150
160
170
180
190
200
210

Fig. 30

Influence of Holes and Slots on Velocity and Mach Number

24 Inch Foil Test Section

⊙ Holes and Slots Closed

× Holes Closed Slots Open

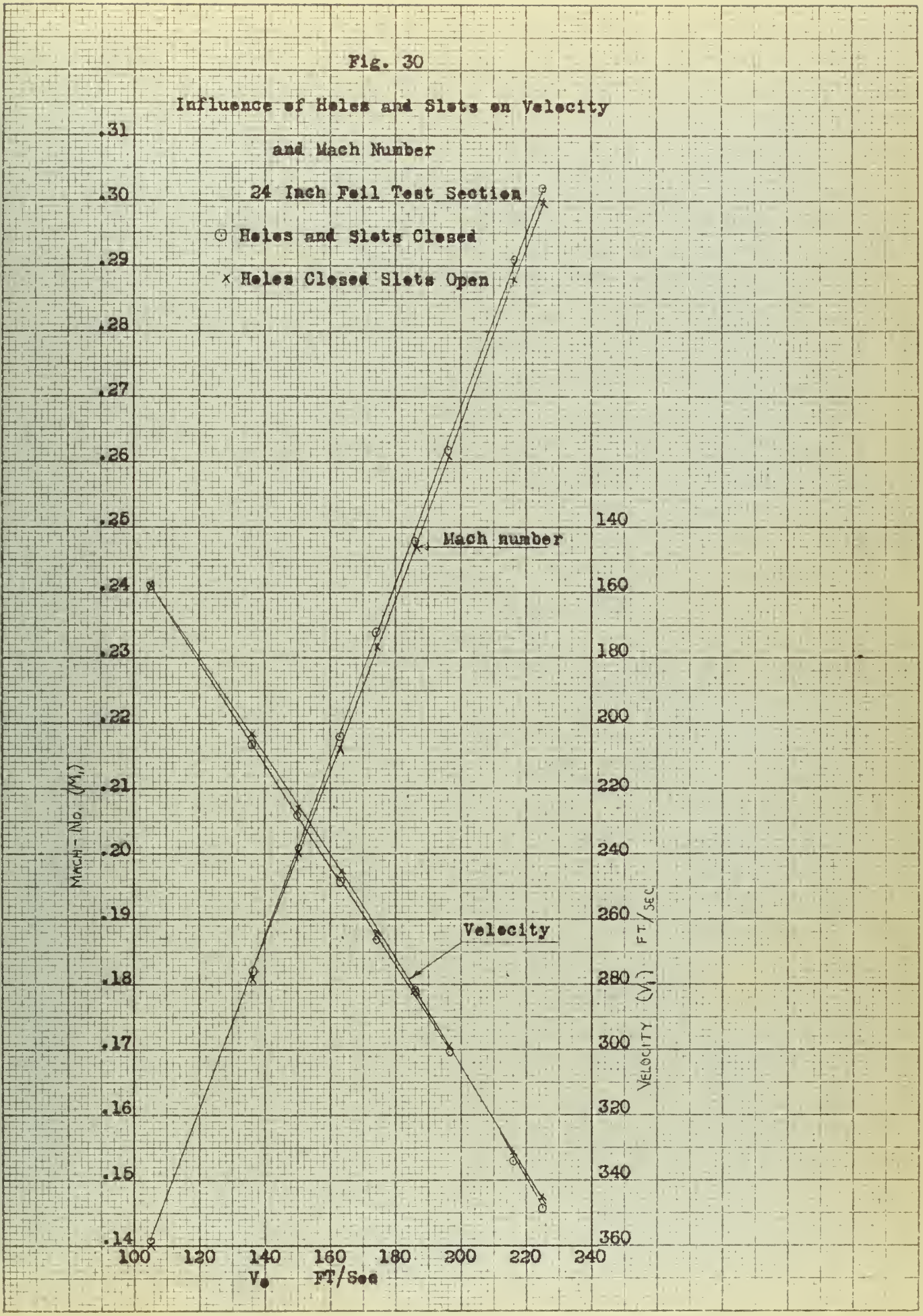

Fig. 31

Velocity and Mach Number Increase Over Incompressible Theory (A_f = 12 inches)

⊙ Experimental Result
× Incompressible Continuity Equation

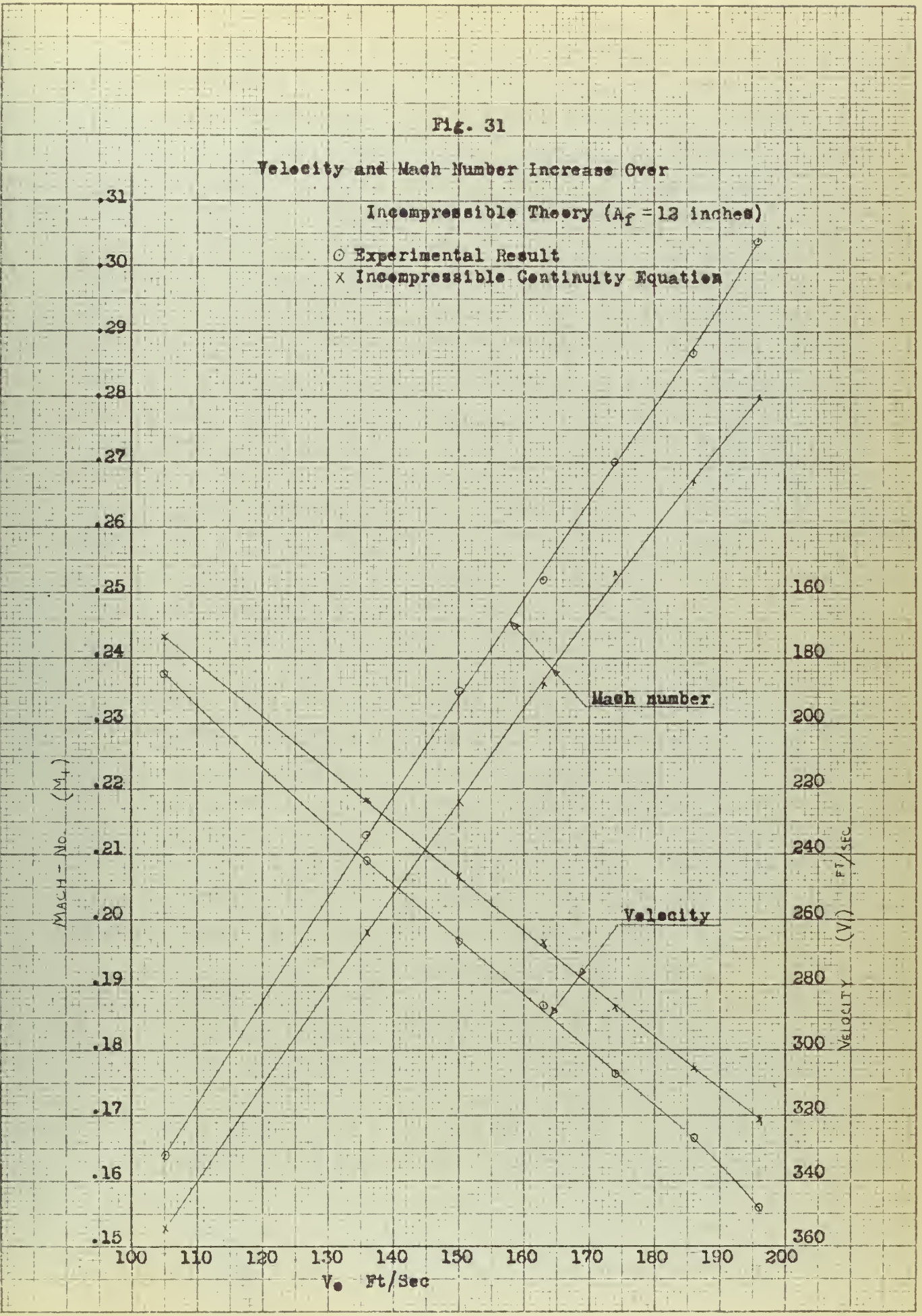

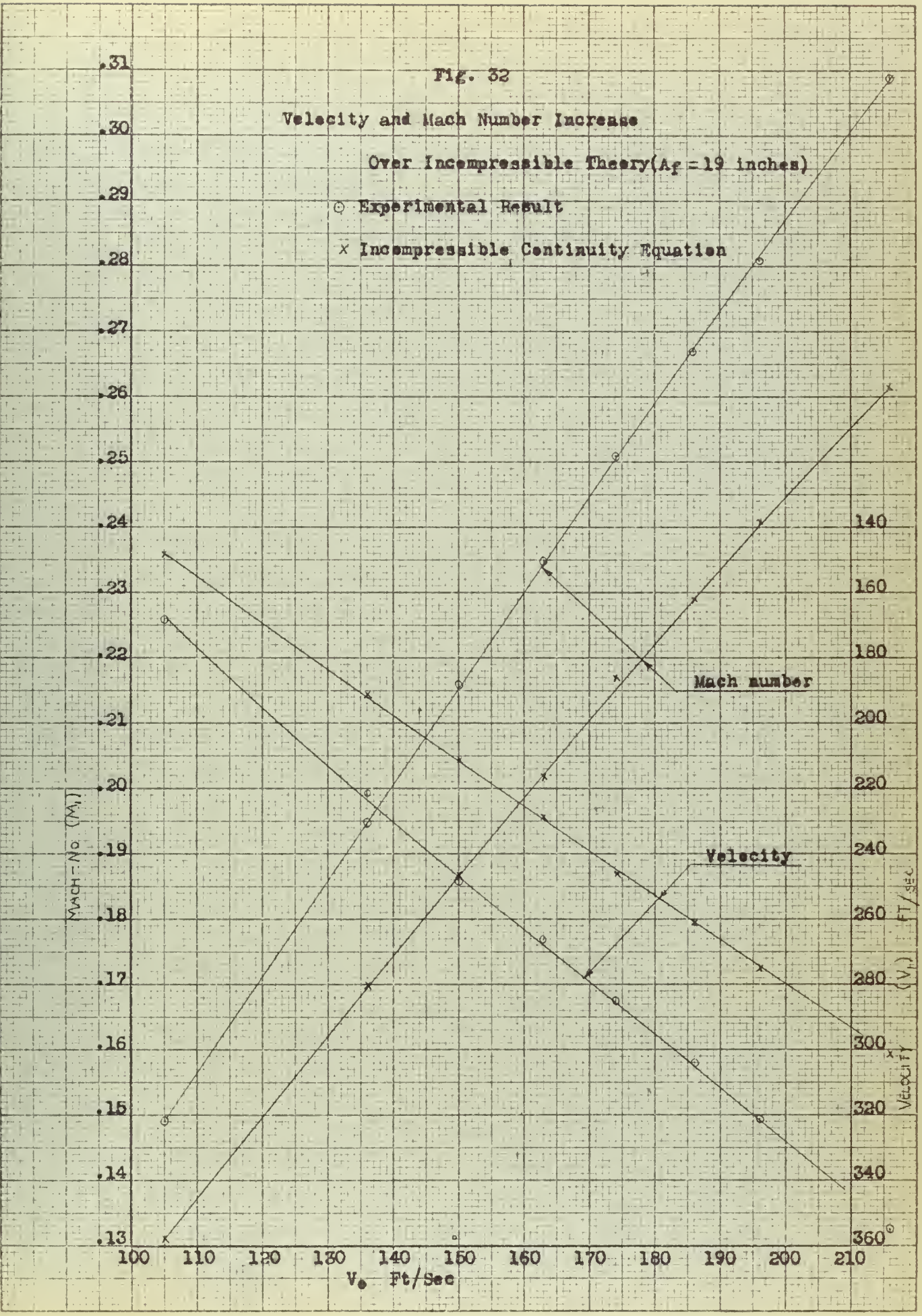
Fig. 32
Velocity and Mach Number Increase
Over Incompressible Theory(A_g = 19 inches)
⊙ Experimental Result
× Incompressible Continuity Equation
Mach number
Velocity
MACH-No (M_1)
VELOCITY (V_1) FT/SEC
V_o Ft/Sec
.31
.30
.29
.28
.27
.26
.25
.24
.23
.22
.21
.20
.19
.18
.17
.16
.15
.14
.13
140
160
180
200
220
240
260
280
300
320
340
360
100
110
120
130
140
150
160
170
180
190
200
210

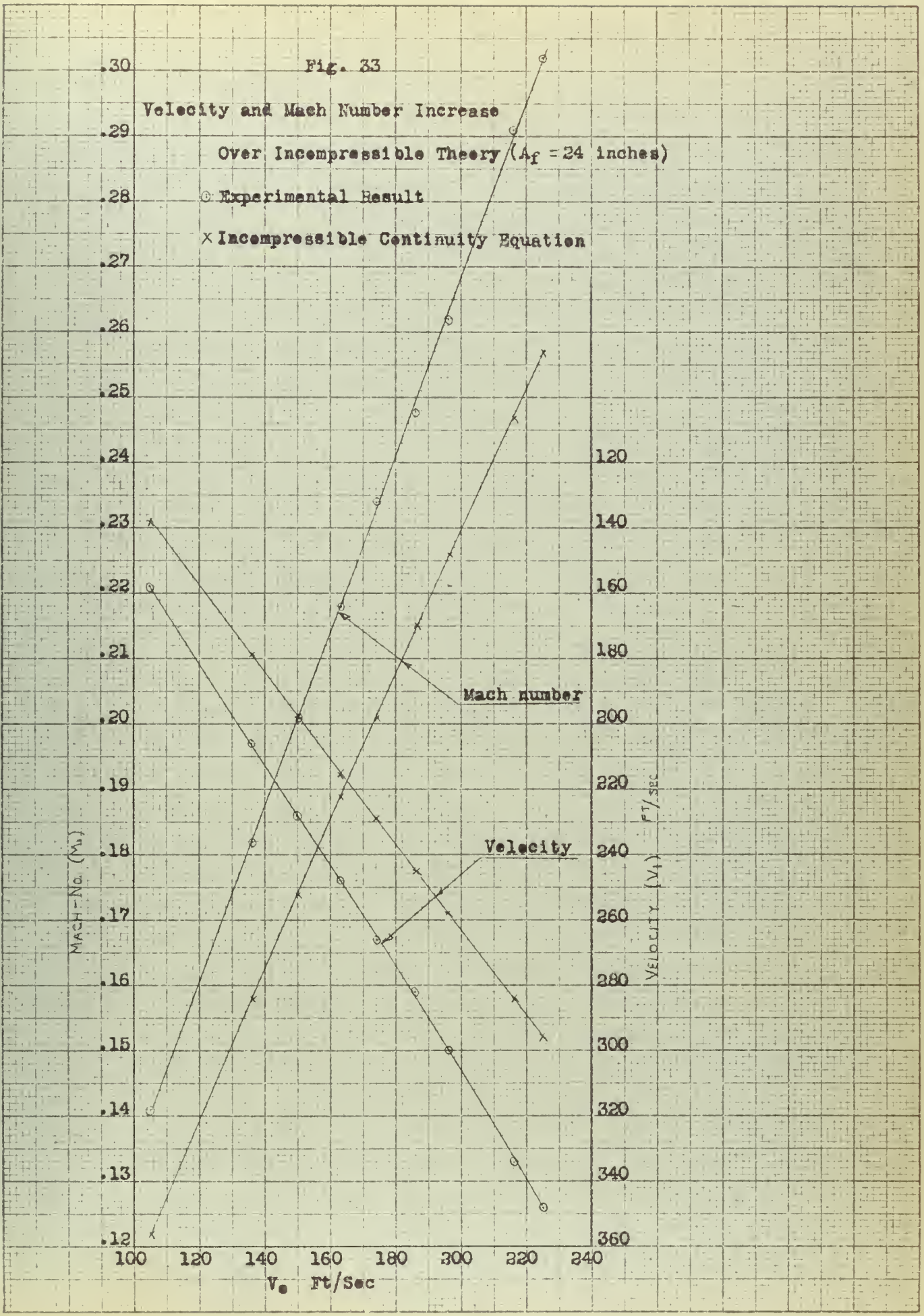
Fig. 33
Velocity and Mach Number Increase
Over Incompressible Theory (A_f = 24 inches)
⊙ Experimental Result
× Incompressible Continuity Equation
Mach number
Velocity
MACH-No. (M_1)
VELOCITY (V_1) FT/SEC
V_o Ft/Sec
.30
.29
.28
.27
.26
.25
.24
.23
.22
.21
.20
.19
.18
.17
.16
.15
.14
.13
.12
120
140
160
180
200
220
240
260
280
300
320
340
360
100
120
140
160
180
300
320
240

Fig. 34

Variation of Maximum Velocity (V_1) and Mach Number (M_1)

with Foil Test Section Width

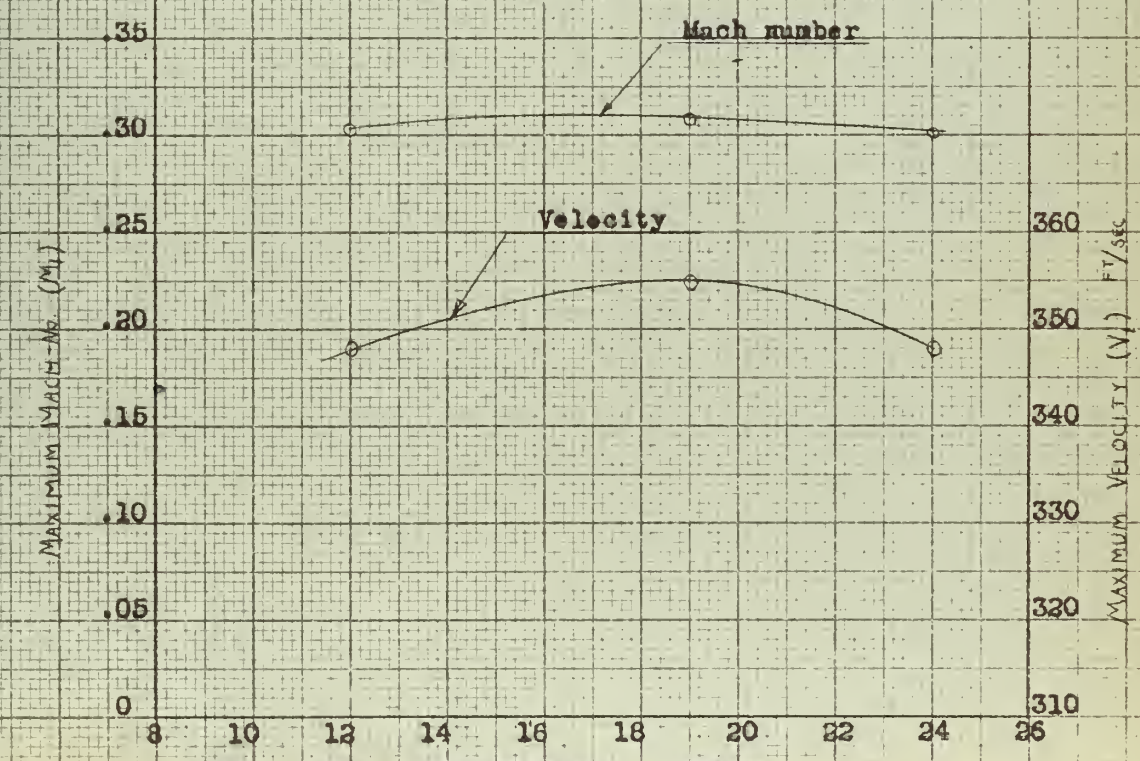

Fig. 35

Mean Percentage Increase of Velocity (V_1) and Mach Number (M_1) over Incompressible Theory

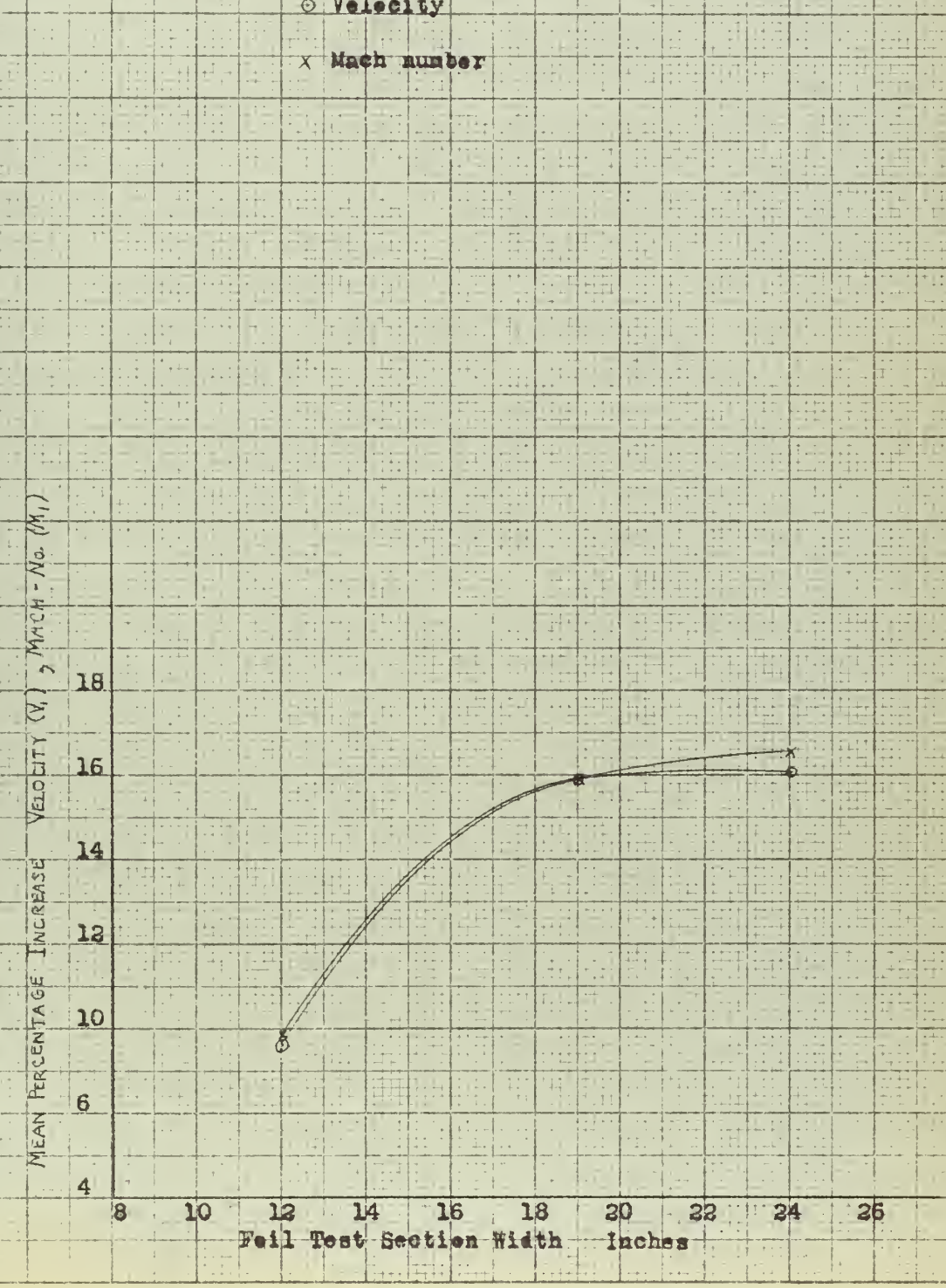

Fig. 36

Variation of Test Section Number with Test Section Width with Increasing Mach Number Importance

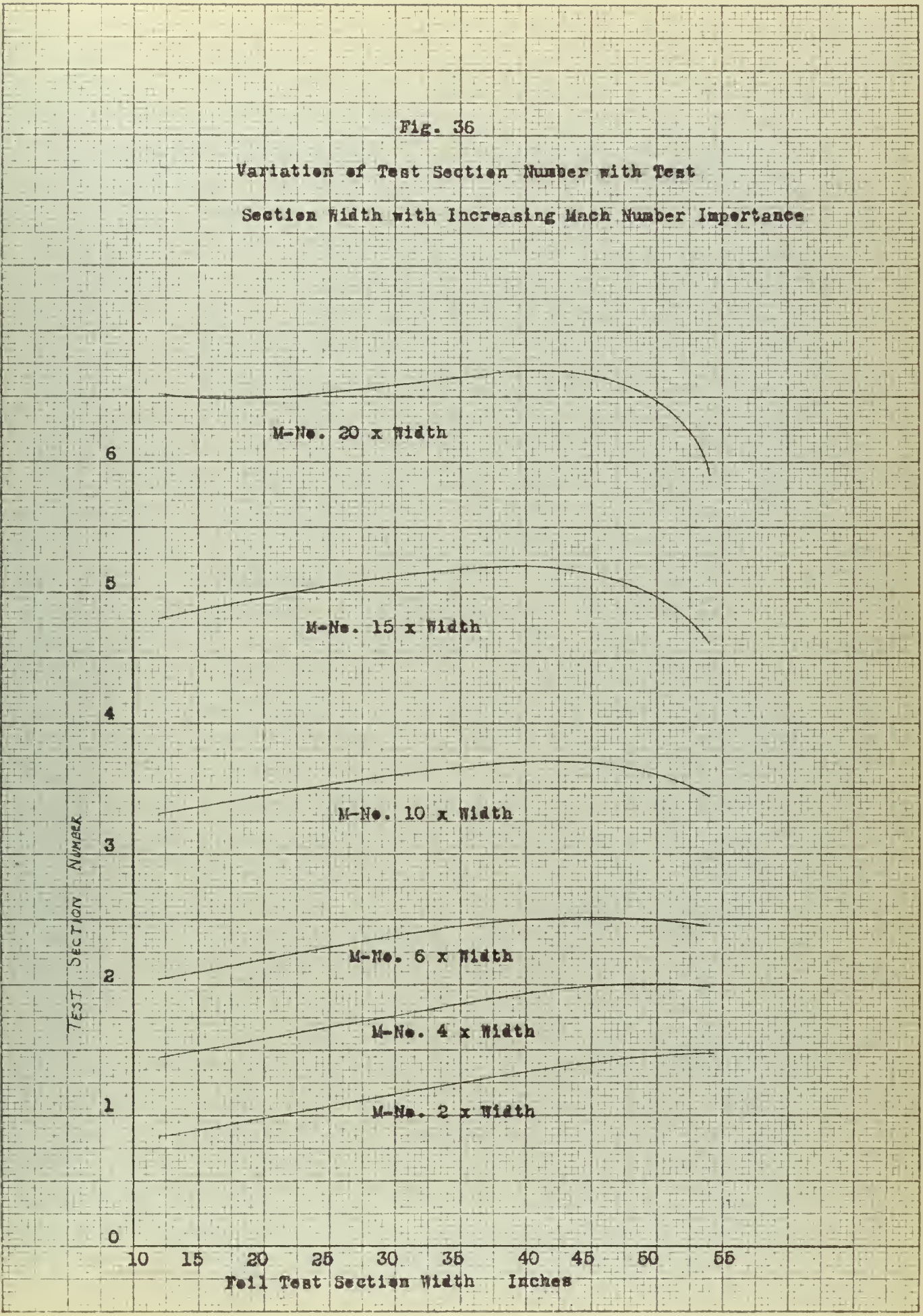

Fig. 37

Velocity Integration

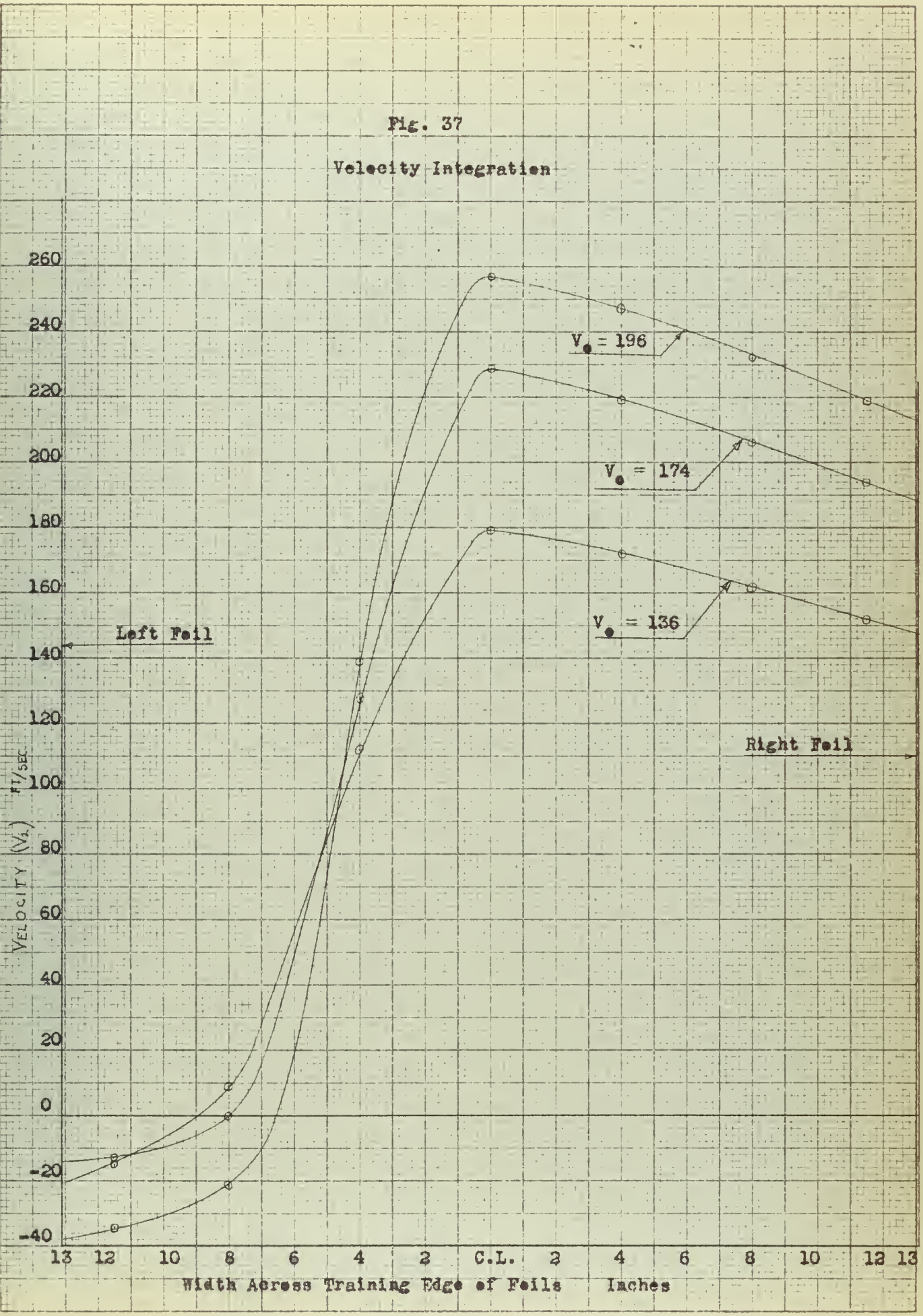

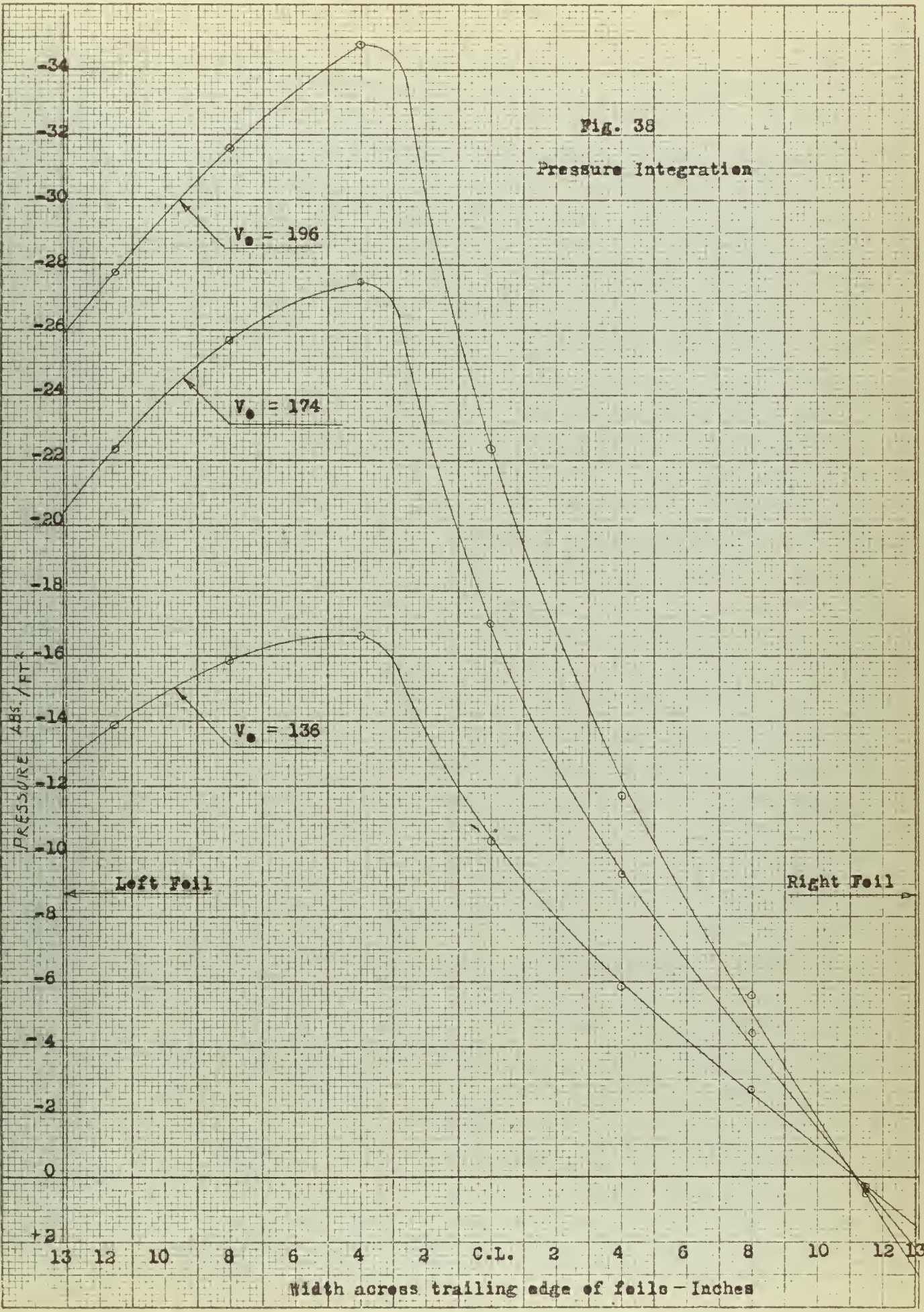

Fig. 38

Pressure Integration

Fig. 39(a)

Result Summary

V_1 maximum Normal Tunnel Test Section 284 Ft/Sec

M_1 maximum Normal Tunnel Test Section .245

Ft/Sec		
V_∞	V_1	M_1
136	242	.213
174	307	.270
196	348	.304

V_∞ maximum

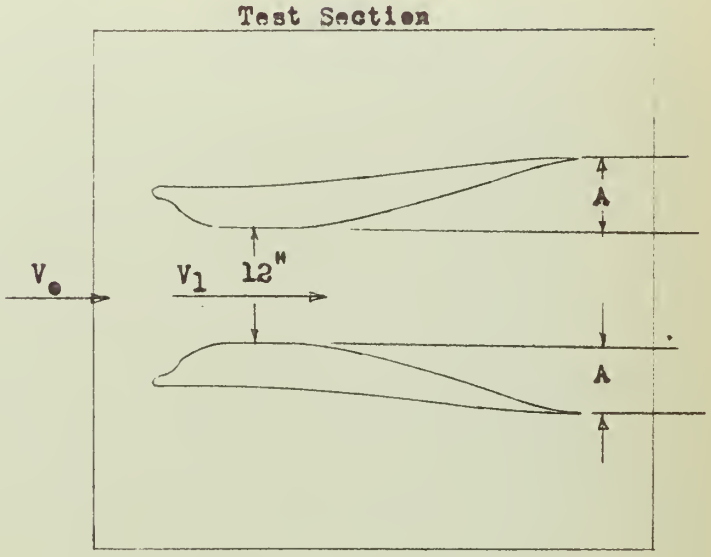

Ft/Sec		
V_∞	V_1	M_1
48.7	209	.184

V_∞ maximum

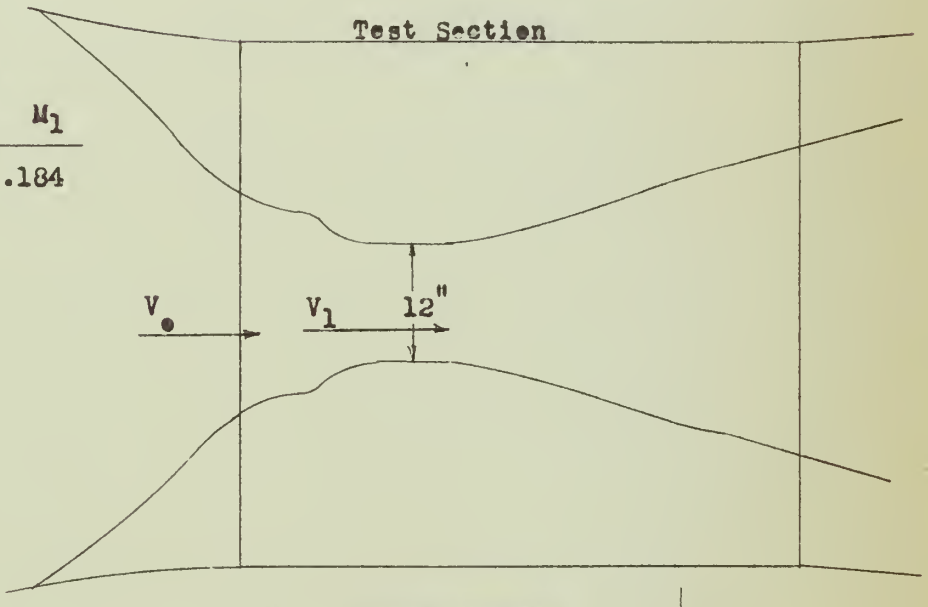

Ft/Sec		
V_∞	V_1	M_1
136	180	.159
174	232	.204
196	262	.228
258	344	.299

V_∞ maximum

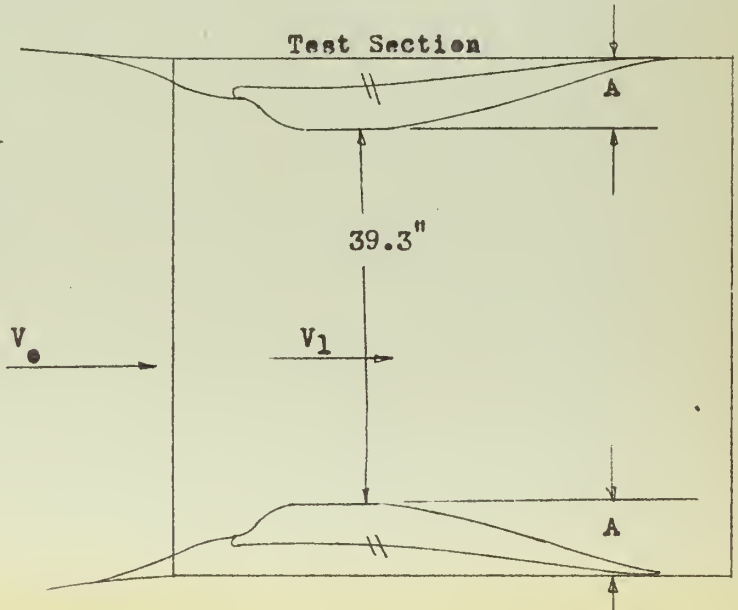

Fig. 39(b)

Result Summary

V_1 maximum Normal Tunnel Test Section = 284 Ft/Sec

M_1 maximum Normal Tunnel Test Section = .245

V_∞ Ft/Sec	V_1	M_1
136	221	.195
174	285	.251
196	321	.281
215	355	.309

V_∞ maximum

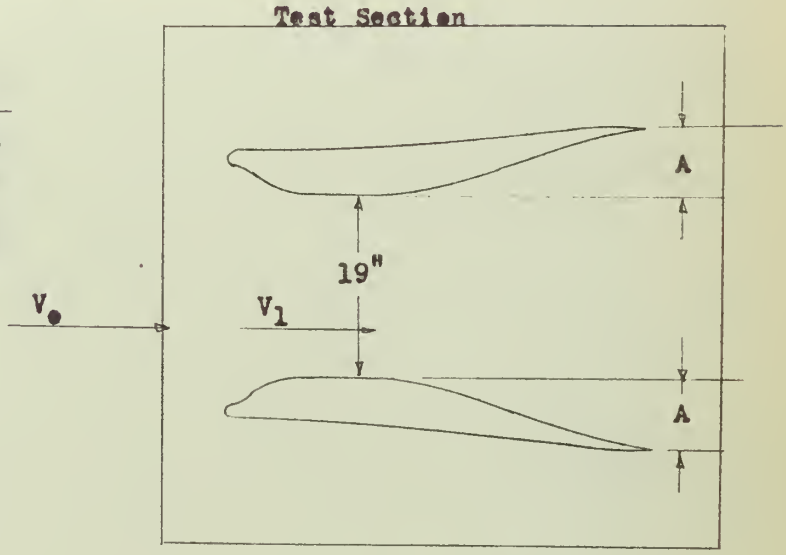

V_∞ Ft/Sec	V_1	M_1
73	204	.180

V_∞ maximum

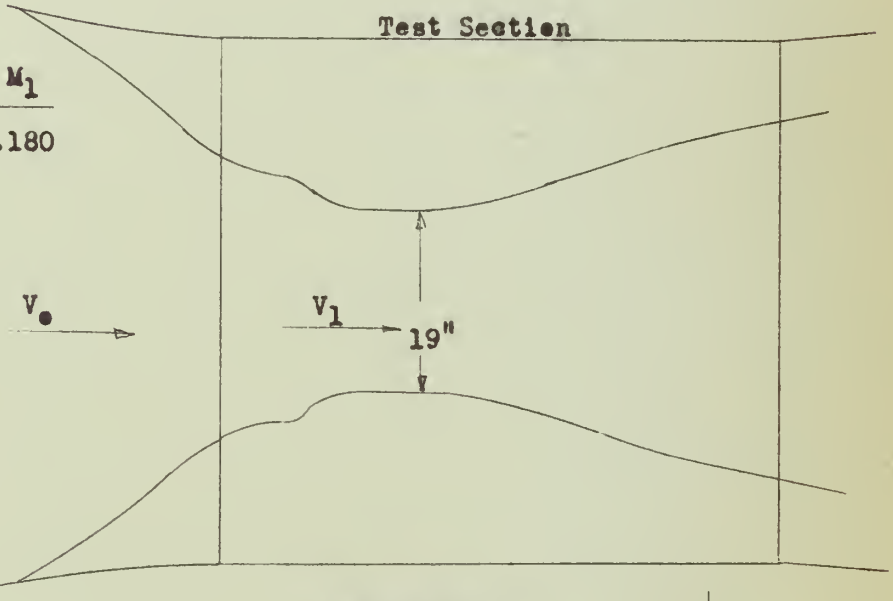

V_∞ Ft/Sec	V_1	M_1
136	180	.159
174	232	.204
196	262	.228
258	344	.299

V_∞ maximum

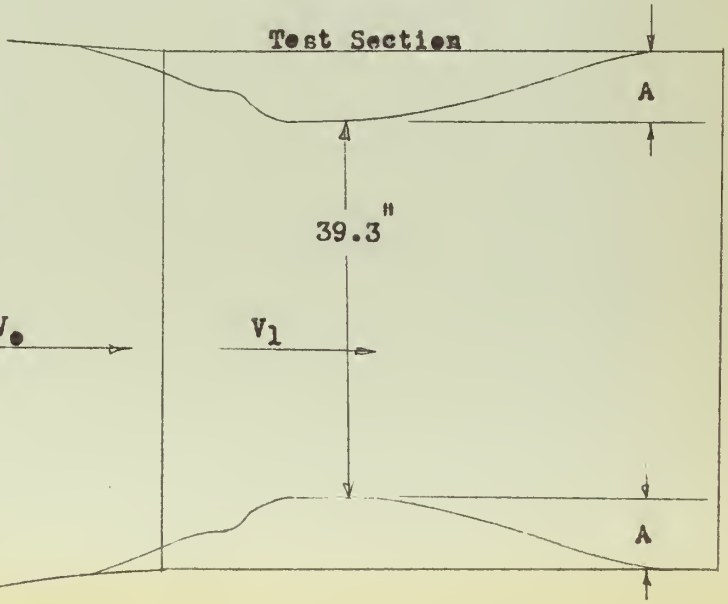

Fig. 39(c)

Result Summary

V_1 maximum Normal Tunnel Test Section = 284 Ft/Sec
M_1 maximum Normal Tunnel Test Section = .245 Ft/Sec

V_∞	Ft/Sec V_1	M_1
136	206	.182
174	266	.234
196	301	.262
225	348	.303

V_∞ maximum

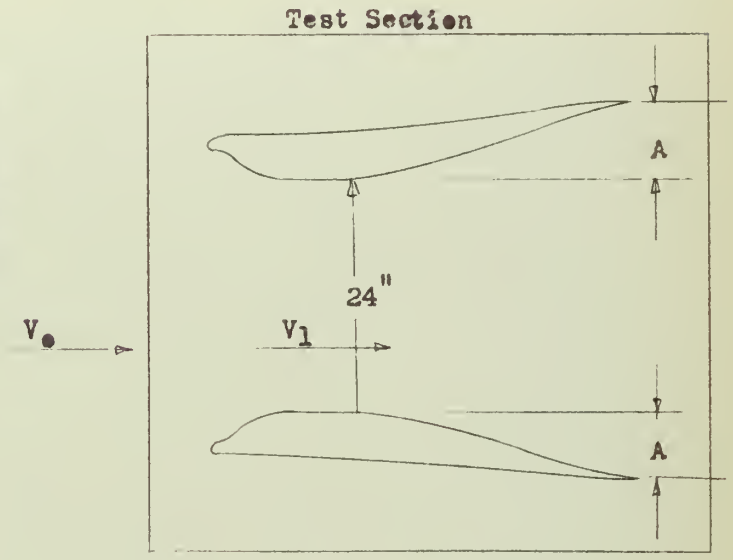

V_∞	Ft/Sec V_1	M_1
100	217	.191

V_∞ maximum

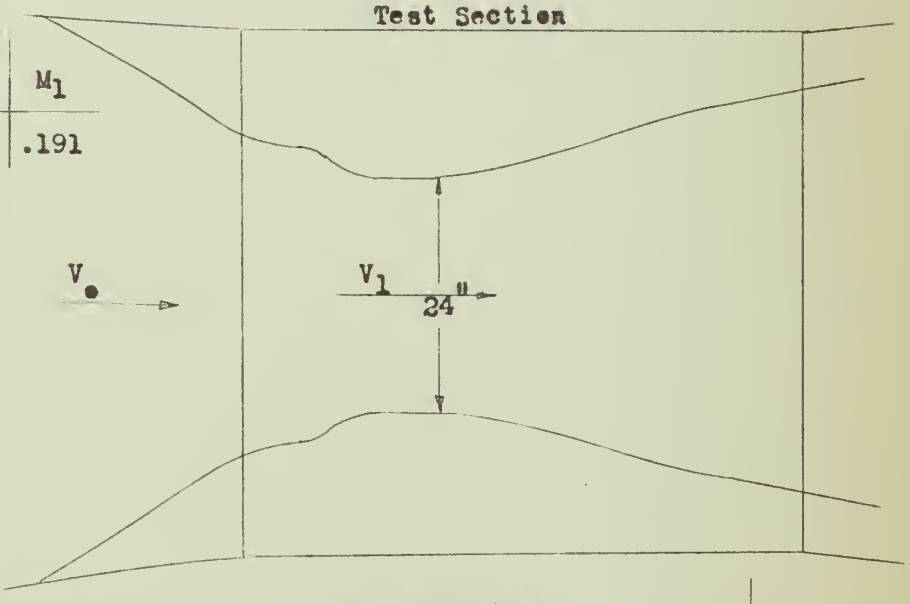

V_∞	Ft/Sec V_1	M_1
136	180	.159
174	232	.204
196	262	.228
258	344	.299

V_∞ maximum

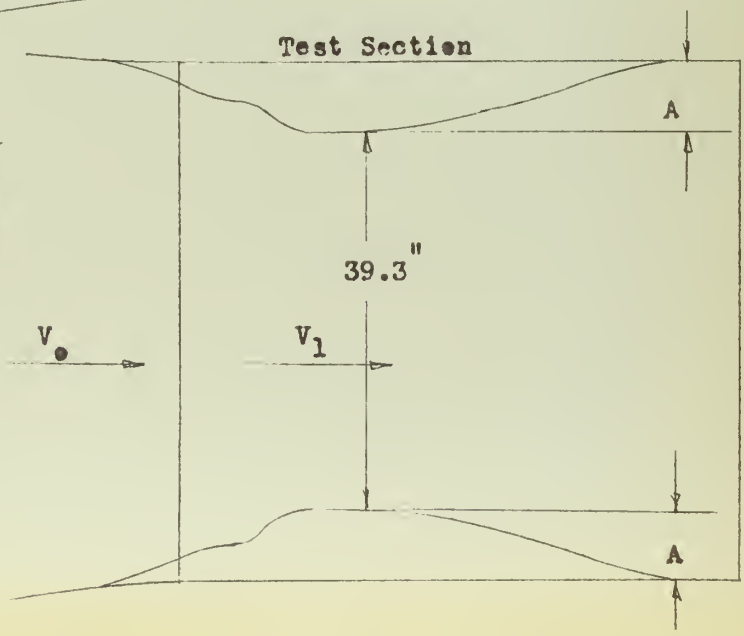

APPENDIX A

Pressure differences across holes and slots by incompressible theory with A_f equal to 24 inches. Pressure differences will be calculated for V_o of 150 Ft/Sec at p static of 2070 Lbs/Ft^2 and total temperature of 80 degrees fahrenheit.

V_o = 150 Ft/Sec

T static = 538 ^oR

p = 2070 Lbs/Ft^2 absolute

p_o = 2070 + q = 2070 + 25 = 2095 Lbs/Ft^2 absolute

p/RT = 2070/(1716)(538) = .00224 Slugs/Ft^3

Exterior Pressures

Contraction Ratios:

Nose of Foils to Holes = 10.2/8.25 = 1.237

Nose of Foils to Slots = 10.2/7.7 = 1.325

Incompressible Continuity Eq: $A_1V_1 = A_2V_2$

$$V_2 = \frac{A_1 V_1}{A_2}$$

V holes = 1.237(150) = 186 Ft/Sec

V slots = 1.325(150) = 199 Ft/Sec

$p_o = p + \frac{\rho}{2} V^2$

p holes = $p_o - \frac{\rho}{2}$ V holes^2 = 2095 - 39 = 2056 Lbs/Ft^2

p slots = 2095 - 44 = 2051 Lbs/Ft^2

Interior Pressures

Nose of Foils to Holes = 15.85/14.7 = 1.078

Nose of Foils to Slots = 15.85/18.25 = .869

V holes = 1.078(150) = 162 Ft/Sec

V slots = .869(150) = 130 Ft/Sec

p holes = $p_o - \frac{\rho}{2} V_{holes}^2 = 2095 - 29 = 2066$ Lbs/Ft^2

p slots = 2095 - 44 = 2051 Lbs/Ft^2

Pressure difference across the holes = 10 Lbs/Ft^2

Pressure difference across the slots = 25 Lbs/Ft^2

APPENDIX B

Data Reduction

Example shown tunnel calibration run(V_o = V tunnel)

Data Recorded

$T_o = 74\ ^oF$

P_o = 17.40 Inches of Alcohol (Sp. Gravity .7962)

P = 20.45 Inches of Alcohol (Sp. Gravity .7962)

P reference = Atmospheric pressure 20.36 Inches of Alcohol (Sp. Gravity .7962)

U-Tube Manometer Difference Inches of red Fluid (Sp. Gravity .834) = 2.88 Inches

Barometer Corrected = 29.108 Inches of Mercury

Reduction of Data

p_o = P ref. - P_o = 20.36 - 17.40 = 2.96 Inches of Alcohol

p = P ref. - p = 20.36 - 20.45 = -.09 Inches of Alcohol

To convert Inches of Alcohol to Lbs/Ft^2:

$2.96(.7962)(5.204) = 12.27$ Lbs/Ft^2 Gage
(5.204 ← Conversion Factor)

$-.09(.7962)(5.204) = .37$ Lbs/Ft^2 Gage

To Convert Inches of Mercury to Lbs/Ft^2:

$29.108(70.73) = 2057$ Lbs/Ft^2
(70.73 ← Conversion Factor)

p_o gage + 2057 = p_o absolute = 2069.27 Lbs/Ft^2 absolute

p gage + 2057 = 2056.63 Lbs/Ft^2 absolute

$q = p_o - p = 2069.27 - 2056.63 = 12.64$ Lbs/Ft^2

$q = M^2 \gamma\ p/2$ (Thermal Perfect)

$M = \sqrt{2q/\gamma p} = \sqrt{2(12.64)/1.4(2056.63)} = .0933$

$T/T_o = (1 + \frac{\gamma-1}{2} M^2)^{-1}$ (Adiabatic Perfect)

$T_o = 74 + 459 = 533\ ^oR$

$T = 533\ ^oR$

$\rho = p/RT = 2056.63/1716(533) = .00225$ Slugs/Ft^3

$q = \frac{\rho}{2} V^2$

$V = \sqrt{2q/\rho} = \sqrt{2(12.64)/.00225} = 105$ Ft/Sec

To Compute V_o

Assume isentropic flow and $p_o = p_o$ in settling chamber.

U-Tube ΔP = Inches of fluid (Sp. Gravity .834)

$2.88(.834)(5.204) = 12.51$ Lbs/Ft^2 = q of V_o

$p_o = 2069.27$ Lbs/Ft^2 absolute

$q = 2069.27 - p = 12.51$ Lbs/Ft^2

$p = 2056.66$ Lbs/Ft^2 absolute

$M = \sqrt{2q/\gamma p} = \sqrt{2(12.51)/1.4(2056.66)} = .09325$

$T_o = 533\ ^oR$

$T = 533\ ^oR$

$\rho = p/RT = 2056.66/1716(533) = .00225$ Slugs/Ft^3

$V = \sqrt{2q/\rho} = \sqrt{2(12.51)/.00225} = 105$ Ft/Sec

APPENDIX C

Modification of Piezometer Pressure Difference when Additional Contraction Accelerates the Flow over the Test Section Piezometer Openings.

12 Inch Foil Test Section

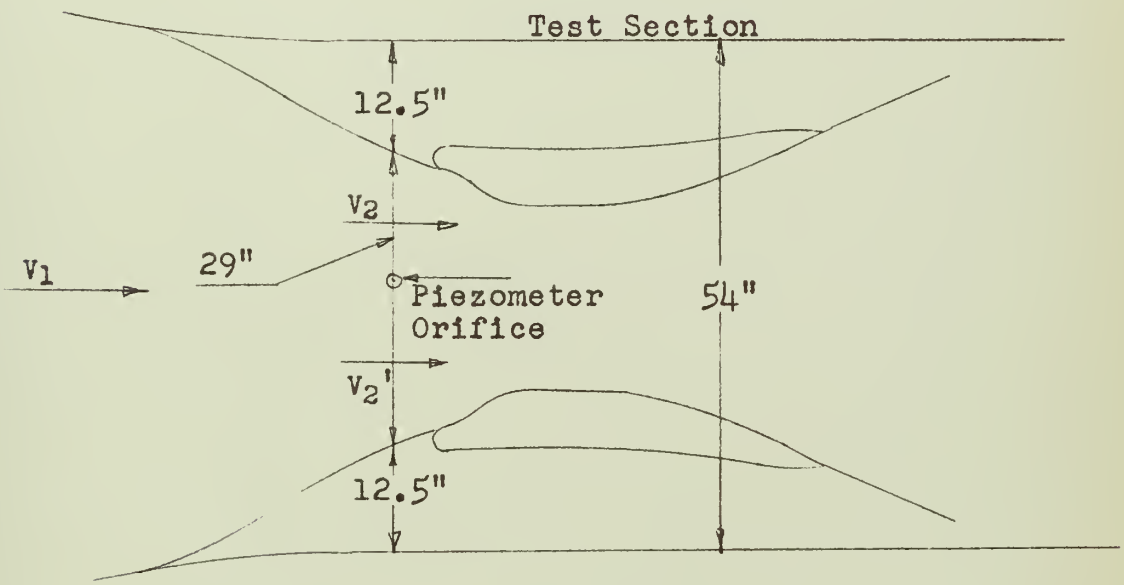

Contraction Ratio: 54/29 = 1.862

V_1 = Velocity in Settling Chamber

V_2 = Velocity before additional contraction was added

V_2' = Velocity after additional contraction was added

$1.862\ V_2 = V_2'$ $\qquad V_2 = V_2'/1.862$

Before Contraction Added:

$$p_o = p_1 + \frac{\rho}{2} V_1^2 = p_2 + \frac{\rho}{2} V_2^2$$

$$p_1 - p_2 = \frac{\rho}{2} (V_2^2 - V_1^2) \qquad V_1 \approx 0$$

$$p_1 - p_2 = \frac{\rho}{2} V_2^2$$

After Contraction Added:

$$p_1 - p_2 = \frac{\rho}{2} (V_2'/1.862)^2$$

$$3.47(p_1 - p_2) = \frac{\rho}{2} V_2'^2 \qquad p_1 - p_2 = 20.90 \text{ Lbs/Ft}^2$$

$$3.47(20.90) = 72.50 \text{ Lbs/Ft}^2 = \Delta P \text{ Piezometer}$$

24 Inch Foil Test Section

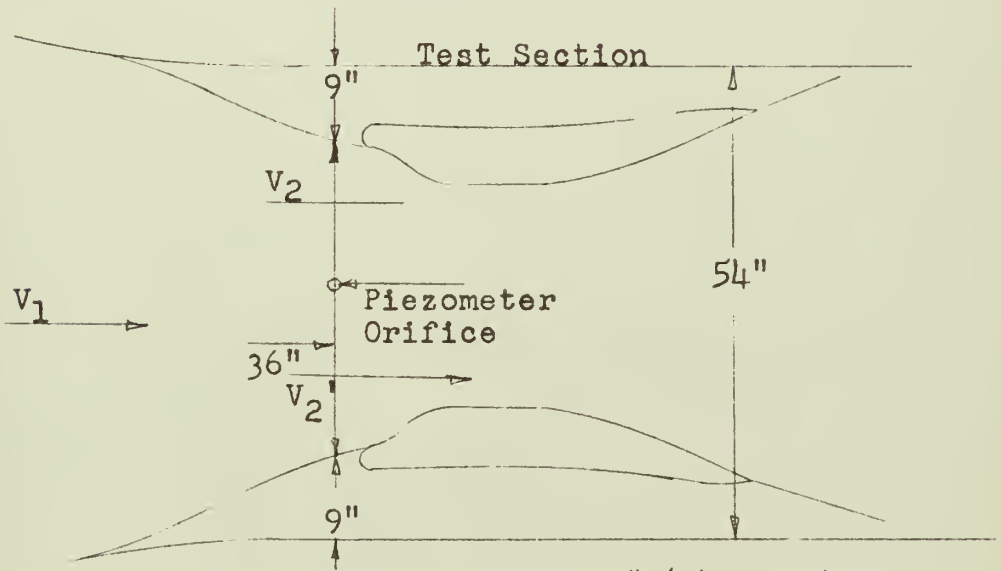

Contraction Ratio: 54/36 = 1.5

$$1.5V_2 = V_2' \qquad V_2 = V_2'/1.5$$

Before Contraction Added:

$$p_1 - p_2 = \frac{\rho}{2} (V_2^2 - V_1^2) \qquad V_1 \approx 0$$

After Contraction Added:

$$p_1 - p_2 = \frac{\rho}{2} (V_2'/1.5)^2$$

$$2.25(p_1 - p_2) = \frac{\rho}{2} V_2'^2$$

$$p_1 - p_2 = 20.90 \text{ Lbs/Ft}^2$$

$$2.25(20.90) = 47.0 \text{ Lbs/Ft}^2 = \Delta P \text{ Piezometer}$$

19 Inch Foil Test Section

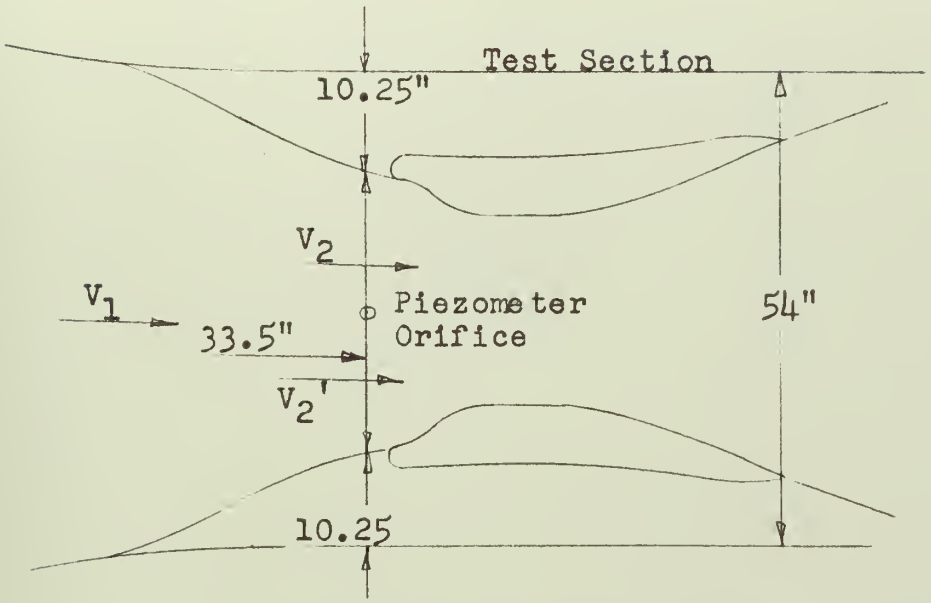

Contraction Ratio: 54/33.5 = 1.611

$1.611\ V_2 = V_2'$ $\qquad V_2 = V_2'/1.611$

Before Contraction Added:

$$p_1 - p_2 = \frac{\rho}{2}(V_2^2 - V_1^2) \qquad V_1 \approx 0$$

After Contraction Added:

$$p_1 - p_2 = \frac{\rho}{2}(V_2'/1.611)^2$$

$$2.6(p_1 - p_2) = \frac{\rho}{2} V_2'^2$$

$$p_1 - p_2 = 20.90 \text{ Lbs/Ft}^2$$

$$2.6(20.90) = 54.40 \text{ Lbs/Ft}^2 = \Delta P \text{ Piezometer}$$

39.3 Inch Foil Test Section (Foils Mounted on Walls)

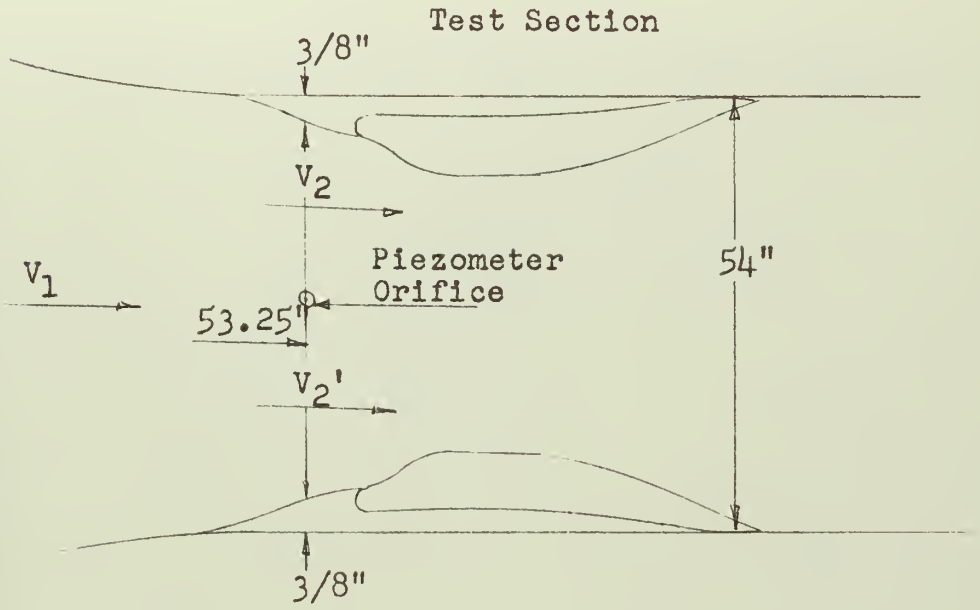

Contraction Ratio: $54/53.25 = 1.014$

$1.014\ V_2 = V_2'$ $\qquad V_2 = V_2'/1.014$

Before Contraction Added:

$$p_1 - p_2 = \frac{\rho}{2}(V_2^2 - V_1^2) \qquad V_1 \approx 0$$

After Contraction Added:

$$p_1 - p_2 = \frac{\rho}{2}(V_2'/1.014)^2$$

$$1.027(p_1 - p_2) = \frac{\rho}{2} V_2'^2$$

$$p_1 - p_2 = 20.90 \text{ Lbs/Ft}^2$$

$$1.027\ (20.9) = 21.5 \text{ Lbs/Ft}^2 = \Delta P \text{ Piezometer}$$

APPENDIX D

Computation of the Velocity of Flow About the Foils

Test Section

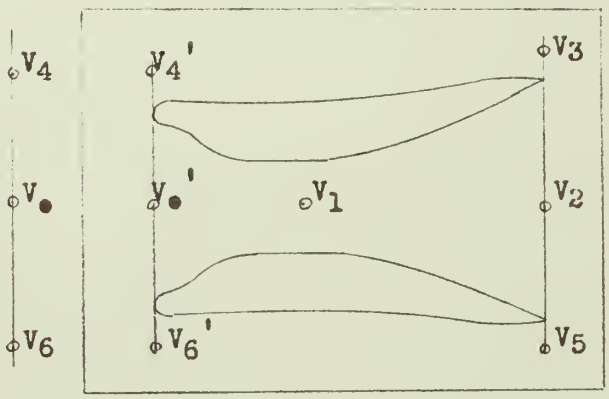

Contraction Ratios:

V_3 to V_4' = V_5 to V_6' = .810

V_2 to V_1 = 2.185

V_1 to V_o' = .610

From Fig. 37, the Integrated V_2 for V_o = 136 Ft/Sec is 114 Ft/Sec

Interior Flow:

$$V_1 = \frac{A_2 V_2}{A_1} = 2.185(114) = 249 \text{ Ft/Sec}$$

$$V_o' = \frac{A_1 V_1}{A_o'} = .610(249) = 152 \text{ Ft/Sec}$$

Exterior Flow:

p exterior = 1.24 Lbs/Ft^2 gage
p interior = .24 Lbs/Ft^2 gage
} mean = .74 Lbs/Ft^2 Assuming pressures will equalize a short distance downstream.

p_o exterior = 27.62 Lbs/Ft^2 gage

$p_o = p + q_3$ $\qquad q_3 = 27.62 - .74 = 26.88$ Lbs/Ft^2

$\rho_3 = 2070/(1716)(534) = .00226$ Slugs/Ft^3

$V_3 = \sqrt{2q/\rho} = 153$ Ft/Sec

$V_4' = \frac{A_3 A_4'}{V_3} = .810(153) = 124$ Ft/Sec

To Calculate V_o

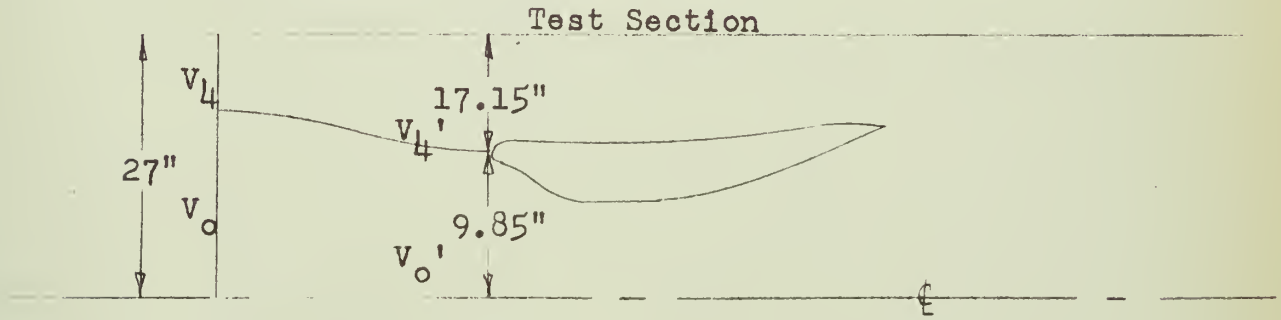

Assume: $V_o = V_4$

$V_o = \frac{A_o' V_o'}{A_o}$ $\qquad V_4 = \frac{A_4' V_4'}{A_4}$

$\frac{A_o' V_o'}{A_o} = \frac{A_4' V_4'}{A_4}$ $\qquad A_o/A_4 = \frac{A_o' V_o'}{A_4' V_4'}$

$A_o + A_4 = 27"$ $\qquad A_o = 27 - A_4$

$\frac{27 - A_4}{A_4} = 27/A_4 - 1$

$27/A_4 = 1 + \frac{A_o' V_o'}{A_4' V_4'}$

$A_4 = 27/1 + \frac{A_o' V_o'}{A_4' V_4'}$

$A_o' = 9.85"$ $\qquad A_4' = 17.15"$

$V_o' = 152$ Ft/Sec $\qquad V_4' = 124$ Ft/Sec

$A_4 = 27/1 + \frac{9.85(152)}{17.15(124)} = 15.85"$

Contraction Ratios:

V_o' to V_o = 9.85/11.15 = .883

V_4' to V_4 = 17.15/15.85 = 1.082

V_o = .883(152) = 134 Ft/Sec

V_4 = 1.082(124) = 134 Ft/Sec

Exterior of Left Foil:

p exterior = -7.96

p interior = -13.83

Weighted mean = -9.91 Lbs/Ft^2

p_o exterior = 26.99 Lbs/Ft^2 Gage

q_5 = 26.99 + 9.91 = 36.90 Lbs/Ft^2

ρ_s = 2070/1716(532) = .00227

$V_5 = \sqrt{2q/\rho}$ = 180 Ft/Sec

$V_6' = \frac{A_6 V_6}{A_6'}$ = .810(180) = 146 Ft/Sec

$A_6 = 27/1 + \frac{A_o' V_o'}{A_6' V_6'} = 27/1 + \frac{9185(152)}{17.15(146)} = 16.90$

A_o = 27 - 16.90 = 10.10

Contraction Ratios:

V_o' to V_o = 9.85/10.10 = .975

V_6' to V_6 = 17.15/16.90 = 1.015

V_o = .975(152) = 148 Ft/Sec

V_6 = 1.015(146) = 148 Ft/Sec

APPENDIX E

Computation of the Incompressible Efficiency of the Diffuser

$$\eta = \frac{p_2 - p_1}{\frac{\rho}{2} V_1^2 (1 - (A_1/A_2)^2)}$$

p_2 will be the Integrated p_2 from Fig. 38.

$V_o = 136$ Ft/Sec

$p_2 = -9.1$ Lbs/Ft^2 gage

$p_1 = -36.20$ Lbs/Ft^2 gage

$V_1 = 242$ Ft/Sec

$= .00221$ Slugs/Ft^3

$A_1/A_2 = .4576$ $\qquad (A_1/A_2)^2 = .21$

$$\eta = \frac{-9.1 + 36.20}{.00221/2\ (242)^2 (1 - .21)} = .531 = 53.1\%$$

Thesis
R689
c.1

35906

Roland

An investigation of a method of increasing the mach number range of a subsonic wind tunnel by means of an internal nozzle in the test section.